

HYDROMODIFICATION EFFECTS ON
FLOW PEAKS AND DURATIONS IN
SOUTHERN CALIFORNIA URBANIZING WATERSHEDS

*Robert J. Hawley
Brian P. Bledsoe
Eric D. Stein*



Southern California Coastal Water Research Project

Technical Report 654 - July 2011

Hydromodification Effects on Flow Peaks and Durations in Southern California Urbanizing Watersheds

Robert J. Hawley^a

Brian P. Bledsoe^b

Eric D. Stein^c

^a *Colorado State University, Department of Civil and Environmental Engineering,
Fort Collins, CO (Presently: Sustainable Streams, Louisville, KY)*

^b *Colorado State University, Department of Civil and Environmental Engineering,
Fort Collins, CO*

^c *Southern California Coastal Water Research Project, Biology Department,
Costa Mesa, CA*

Technical Report 654

July 2011

Executive Summary

A critical first step to hydromodification management is quantifying the effects of watershed urbanization on both flow peaks and flow durations. This report provides an analysis of forty-three regional U. S. Geological Survey gauges with records greater than ~20 yrs located in watersheds ranging from 1.3 – 272 km². The goal was to quantify effects of hydromodification, and to develop regionally calibrated, empirically derived models that can be applied to ungauged streams throughout southern California. The study watersheds spanned a gradient of urban development and ranged from 0 to 23% total impervious area based on 2001 land use data. With little flow control at the subdivision scale to date, most of the region’s impervious area is hydrologically effective, in that it is relatively well-connected to surface-drainage networks. Consequently, total impervious area was an effective hydrologic surrogate for urbanization.

Large increases were observed in instantaneous-peak flows of more frequent return periods (e.g., 1.5 and 2 year storms), with greater than a 5-fold increase in 2-year events (Q_2) observed in a watershed with 20% imperviousness relative to \leq ~1% imperviousness (Table ES-1). Effects of urbanization decreased for larger, less frequent storms. For example, 20% impervious cover resulted in a 40% increase in 10-year peak flows. Such attenuating influence of urbanization with return period is generally consistent with both theory and previous studies (Bledsoe and Watson, 2001; Hollis, 1975; Sauer *et al.*, 1983). During very large, infrequent events (e.g., Q_{100}) soils become saturated and behave similar to impervious surfaces; therefore, urbanization effects can be difficult to detect.

Table ES-1. Influence of urbanization (as measured by total impervious area) on peak-flow rates.

Flow	Peak Factors ^(a) for Impervious Extent, Imp _{max}					Factor Range at 20% Impervious	
	1%	5%	10%	15%	20%	Minimum	Maximum
$Q_{1.5}$	x 1.1	1.8	3.2	5.7	9.8	6.3	13.6
Q_2	x 1.1	1.5	2.4	3.6	5.6	3.8	7.3
Q_5	x 1	1.2	1.4	1.6	1.9	1	2.2
Q_{10}	x 1	1	1	1	1	1	1.4
Q_{25}	x 1	1	1	1	1	1	1

^(a) 'typical' factors (i.e., median influence factors of all five sets of Q_i equations)

Effects of hydromodification on flow duration were expressed as duration density functions (DDFs), which are generally defined as the number of days that exceed a given flow. They are conceptually similar to probability density functions for logarithmically-binned mean daily discharges greater than some nominal value, for example 1 to 10 cubic feet per second (0.03 to 0.3 m³/s), depending on watershed size.

The results of this study show that for a particular watershed size and climatic setting, urbanization resulted in proportionally-longer durations of all geomorphically-effective flows, with a more pronounced effect on the durations of low to moderate flows. For example, an average watershed from the study area with ~15% imperviousness could experience three to four times as many days of moderate flows (~100 cfs) and greater than 2-fold duration increases for even the largest flows (~1,000 cfs) relative to an undeveloped setting (i.e., ~1% imperviousness, Figure ES-1). These empirical findings of decreasing influence of urbanization on flow duration with increasing flow magnitude are consistent with the findings regarding peak flows: urbanization tends to show higher influence on more frequent events, with decreasing influence over the largest, rarest storms.

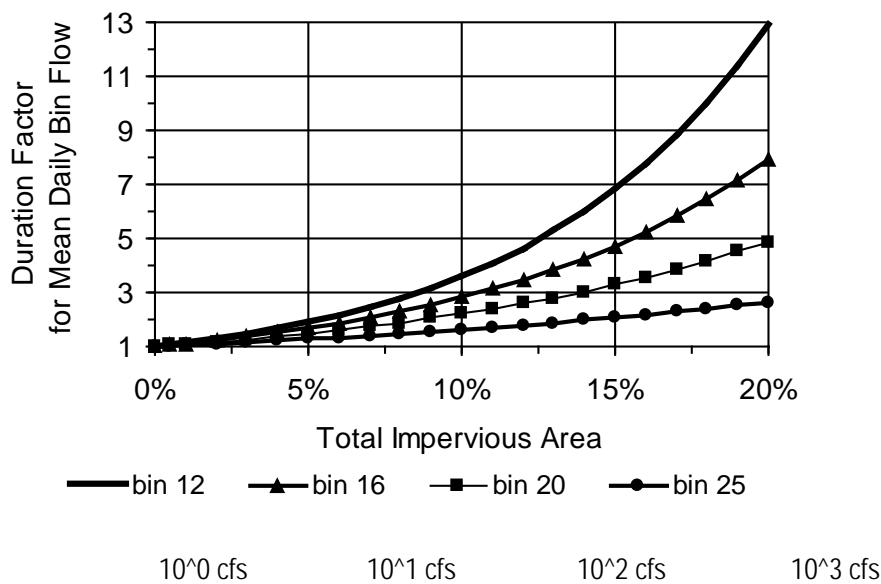


Figure ES-1: Duration factors of respective flow magnitudes across a gradient of Total Impervious Cover based on a 25-year DDF simulations of an average watershed; Average Watershed: A = 25 mi² and P = 25 in.

The models presented in this report may be used to estimate the effects of unmitigated urbanization on flow peaks and flow durations as a part of regional hydromodification management programs. They could be incorporated into screening tools for hydromodification susceptibility (e.g., Bledsoe *et al.*, 2010). They could also serve as a relatively simple, first step in a modeling tool framework prior to employing more sophisticated modeling techniques such as continuous flow simulations based on different landuse and stormwater management scenarios.

The following report includes methodological background and justifications for the development of a suite of models that predict instantaneous peak flows (as an alternative to the existing USGS regional equations (Waananen and Crippen, 1977)), and duration density functions. The report also includes a summary of landuse and climatic histories, and regional geomorphic relationships such as drainage

density vs. annual precipitation and main channel length vs. drainage area. The report concludes with a detailed case study of two gauged watersheds spanning relatively equal periods of pre-urban and post-urban periods, along with a cross-comparison to a proximate reference watershed that remained entirely undeveloped for an identical period of operation. The at-a-station case study, combined with the empirical models, presents a weight of evidence that urbanization has a pronounced and statistically-significant influence on flow magnitudes and durations of southern California stream networks.

Acknowledgements

We would like to thank organizations and individuals who contributed to this project in terms of funding, data collection, and analysis. This research was funded in part by a State of California research grant, for which we are very grateful. Becky Schaffner of SCCWRP was extremely helpful in providing GIS assistance and training. The USGS continues to deliver spatial and hydrologic data to the public domain that are unparalleled in terms of scale and quality. We would like to extend our gratitude to all staff (past and present), and particularly to Scott Patterson of the South Poway Field Office whose time and care in answering questions provided clarity regarding individual gauges. This document is much improved as a result.

Table of Contents

Executive Summary	i
Acknowledgements	iv
List of Figures	vi
List of Tables	vii
Introduction	1
Research Foundations and Justification	2
Toward Cumulative Durations	2
Study Domain	3
Methods	5
Unit Disclaimer.....	5
Gauge-Selection Criteria	5
Instantaneous Peak Flows	10
Long-Term Cumulative Durations.....	12
Measures of Urbanization.....	15
Other Physically-Based Metrics.....	20
Analytical Methods and Model Design	24
Results	26
Cross-Validation Summaries and Individual Variable Performance.....	26
Peak-Flow Equations.....	30
Duration Density Functions	36
Implications and Discussion	40
Effects of Urbanization Predicted by Models.....	40
Summary and Conclusions.....	48
Future Work	49
References	50
Internet References – GIS Data Sources	54

List of Figures

Figure 1. Locations of gauges used in equation development ('wet' subset) with corresponding watershed and main channel, overlaid by a gradient of imperviousness and county boundaries, with rural (Hopper) and urban (Arroyo Simi) case study gauges.	6
Figure 2. Flow versus recurrence interval of 30-yr record at USGS gauge no. 11033000, West Fork San Luis Rey River near Warner Springs, California, with Log-Pearson Type III adjusted ($Q + 0.1$) and ($Q + 100$) and inverse gamma distributions, and log-transform function.	11
Figure 3. DDFs of gauges De Luz and San Antonio fitted to centroids of logarithmically distributed histogram bins 16-25 with selected variables of drainage area (A), average annual precipitation (P), and record length (Yr).	14
Figure 4. 2001 imperviousness and road vectors tracked through time per USGS historic quadrangle maps and current Cal-Atlas shapefiles at Arroyo Trabuco (Orange County, California, near intersection of Interstates 5 and 405).	17
Figure 5. Imperviousness and road density through time at Arroyo Trabuco, overlaid by active gauge years and linear regression of imperviousness (Imp) as a function of calendar year (CY) from 1967 to 2001.	18
Figure 6. Exponential correlation between impervious area in 2001 (Imp01) and road density in 2000 (RD00) across all sites.	19
Figure 7. Inter-annual precipitation variability recorded at Los Angeles and San Diego overlaid with number of active gauges and number of gauged watersheds exceeding specified road-density levels (indicating increasing urbanization).	22
Figure 8. Mean spatial extent of road density overlaid by relative difference from long-term mean-annual precipitation recorded at Los Angeles and San Diego during gauge records... 22	22
Figure 9. Main-channel length to basin divide (L) versus drainage area (A): southern California and the Hack (1957) relationship from Maryland and Virginia.	23
Figure 10. Drainage density versus area-averaged mean-annual precipitation.	24
Figure 11. Cross-validation performance of $Q_i = f(\text{Stm}, P_{224})$ for 25-yr return interval (predicted Q_{25} versus actual) with 1:1 'perfect-fit' line overlaid.	27
Figure 12. Comparison of performance between Eq. (9) and USGS rural (1977).	35
Figure 13. Comparison of performance between Eq. (9) and USGS urban (1983) in most urbanized watersheds.	36
Figure 14. Peak factors for instantaneous peak flows as a function of TIA for all five calibrated peak flow models: (a) at $Q_{1.5}$, (b) at Q_2 , (c) at Q_5 , (d) at Q_{10}	41

List of Tables

Table 1. Selected ^(a,b) gradients of the forty-three USGS gauged watersheds used to develop models (i.e., model-application bounds), and the nine hydrogeomorphically-distinct gauges ^(c) that were withheld from models.	7
Table 2. Summary of variables tested in models with corresponding significance.....	20
Table 3. Summary of cross-validated models.....	26
Table 4. Corresponding parameters, units, and performance measures for equations.	31
Table 5. Comparison of Q_i model performance with USGS rural (1977) and urban (1983) equations using Standard Error values from arithmetic space.....	36

Introduction

By decreasing infiltration and increasing direct runoff, impervious surfaces can create larger peaks, less groundwater recharge, and increased variability, especially if stormwater is routed directly to streams. These fundamental hydrologic interrelations, such as larger peaks and increased flashiness, have been demonstrated regionally (Galster *et al.*, 2006; Konrad and Booth, 2002) and on a national scale using United States Geological Survey (USGS) gauge data (Poff *et al.*, 2006; Sauer *et al.*, 1983). In California, increased peak flows in developed watersheds have been documented by the USGS as early as 1963 (Waananen, 1969). Durbin (1974) reported potential increases in the 2-yr flow (Q_2) of 3- to 6-fold in San Bernardino County, with little effect on higher return intervals such as the 50-yr flow. Rantz (1971) used development extent and percentage of channels sewerred to estimate peak factors for the San Francisco Bay area ranging from 1 to 4 for Q_2 , and decreasing with larger return intervals (e.g., 1 to 2.5 for Q_{50}).

Such changes in flow, broadly associated with urbanization, are documented as having profound effects on biologic and geomorphic processes, so much so that the U.S. Environmental Protection Agency (EPA) has recently begun to mandate 'hydromodification' regulations (EPA, 2006). Channel instability and complex responses have been associated with urbanization across hydroclimatic regimes (Bledsoe and Watson, 2001; Booth, 1990; Chin, 2006; Chin and Gregory, 2001; Simon and Downs, 1995; Trimble, 1997), while altered flow and sediment regimes affect aquatic life cycles, habitats, food webs, and facilitate colonization by invasive species, among other types of degradation (Poff *et al.*, 2006; Roesner and Bledsoe, 2002; Waters, 1995).

Our recent field investigations in southern California seem to indicate a relatively high geomorphic sensitivity to hydromodification (Hawley, 2009), consistent with previous studies (Coleman *et al.*, 2005) and the semiarid climate in general (Trimble, 1997). The hydrogeomorphic setting (i.e., steep topography, flashy regimes, high-sediment loads, and largely nonresistant bed material) generally compounds risk factors for far-reaching channel responses such as headcutting, extensive mass-wasting, and planform shifts.

An important first step in any hydromodification management program is to quantify the effects of hydromodification on both peak flows and durations (*sensu* Wolman and Miller, 1960). The challenges in quantifying effects are 1) how to determine the most effective flow magnitudes to manage (i.e., which flow magnitudes are most affected by hydromodification); and 2) how to integrate effects on flow duration (i.e., which flow magnitudes perform the most cumulative work on the channel boundary). This report addresses these issues via the following objectives:

1. offer an updated alternative to the USGS (Waananen and Crippen, 1977) regional equations for estimating peak flows of ungauged streams that is calibrated with more recent southern California gage data;
2. develop a physically-based empirical method for estimating long-term cumulative flow duration histograms for ungauged sites; and
3. determine how urbanization affects peak flows and cumulative durations for all geomorphically-important flows by including urban components (if statistically significant) in Objectives 1 and 2.

In filling these knowledge gaps, we offer the following hypotheses:

- H₀: urban influence on the magnitudes of peak flows will be highest at the more frequent events and lowest at the longer recurrence intervals;
- H₀: the lack of representation of southern California gauges used to develop the USGS national urban equation (Sauer *et al.*, 1983) should result in better performance by models calibrated directly to the region; and
- H₀: cumulative durations can be modeled with reasonable accuracies and will be significantly influenced by urbanization.

Research Foundations and Justification

This paper principally builds on the work and ongoing data collection of the USGS. To this day, Waananen and Crippen's (1977) simple power functions of drainage area and mean annual precipitation serve as a primary method of peak-flow estimation in southern California. Limited by an overall lack of gauge data on "streams with drainage areas generally less than 25 mi², and particularly less than 10 mi²," the models came with substantial standard errors and were deemed "generally applicable for streams with drainage areas greater than 10 mi²" (Waananen and Crippen, 1977).

Given over 30 more years of data, and especially more data on smaller streams, it was prudent to revisit these equations. In this paper, we go beyond the Log-Pearson Type III distribution to a more regionally-appropriate statistical distribution. With several gauges in developed watersheds, urbanization was included in the models using direct measures of total impervious area (TIA). This approach is arguably less subjective and more parsimonious than the USGS national approach to urban flow augmentation (Sauer *et al.*, 1983), which can be time intensive and is subject to user interpretation of "basin development factors" that are typically immeasurable with available Geographic Information System (GIS) data. Moreover, of the 199 gauges used to develop the national equations, few gauges were from semiarid settings, with only one from southern California (San Diego Creek, gauge no. 11048500). Despite largely-different hydrologic behavior relative to much of the rest of the nation, the USGS national equations are currently being applied throughout the region.

Toward Cumulative Durations

Peak flows alone can be useful in understanding potential erosive energy at an individual recurrence interval; however, they have less meaning when considered independent of durations. Whether a large flow lasts for minutes or days, it has substantial implications for cumulative sediment transport. Moreover, all flows capable of moving sediment have the potential to influence channel form, *sensu* the concept of geomorphic *effectiveness* (Wolman and Miller, 1960).

It follows that when evaluating the potential impacts of urbanization on channel stability, researchers have begun to favor cumulative sediment-transport models based on continuous or cumulative flows over extended periods (e.g., years/decades). In evaluating various flow-control schemes in the Pacific Northwest, Booth and Jackson (1997) touted the potential benefits of 'duration' standards in contrast to

'peak' standards, particularly at flows above the threshold of sediment entrainment. Consideration of all sediment-transporting flows would seem especially important in the semiarid environment known for sporadic sediment movements (Graf, 1981, 1988), extended periods of aggradation/degradation and lagged recovery times (Wolman and Gerson, 1978), and relatively infrequent periods of equilibrium (Bull, 1997). One of the only published approaches to addressing hydromodification in California to date uses flow-duration histograms produced from long-term rainfall-runoff simulations in Hydrologic Engineering Center - Hydrologic Modeling System (HEC-HMS) to compute an 'effective work index' by summing excess shear stress over cumulative flow durations of 50 yrs (Santa Clara, 2004). The corresponding mitigation goal is to design flow control such that cumulative post-developed sediment-transport capacity matches the pre-developed regime. The Sediment Impact Analysis Method (SIAM), publicly available via the U. S. Army Corps of Engineers (USACE) in the Hydrologic Engineering Center - River Analysis System (HEC-RAS) software package, is also designed to use a histogram-style flow-duration curve and can be used to model long-term sediment transport (Mooney, 2007; USACE, 2009).

An alternative to solely using rainfall-runoff models to develop flow-frequency curves is to base them on local gauge data. Using the nearest upstream/downstream gauge (Hey, 1975) or a gauge from a similar watershed, frequency curves have typically been scaled using a nondimensional index such as Q/Q_{bankfull} (Emmett, 1975; Leopold, 1994) or Q/Q_2 (Watson *et al.*, 1997). The advantage of the latter is that the 2-yr flow may be estimated by a USGS regional equation, whereas the bankfull flow is often difficult to define and does not have a consistent return interval across different streams (Biedenbarn *et al.*, 2000, 2001; Pickup and Warner, 1976; Williams, 1978). The disadvantage of scaling based on the 2-yr flow is that, at least in southern California, it comes with much poorer accuracies than higher recurrence intervals (Waananen and Crippen, 1977). It may also be difficult to define which gauge(s) is similar enough to the ungauged watershed for direct scaling (e.g., similar topography, basin size, precipitation).

We expand on the Watson *et al.* (1997) approach by developing a statistical model to estimate flow-duration curves for ungauged sites with all regional gauges meeting our selection criteria, such that a synthetic flow-duration histogram is predicted as a function of watershed-scale physical descriptors such as drainage area and precipitation. The resulting *conditional* probability density functions that predict cumulative durations of geomorphically-effective flows in a histogram format are henceforth referred to as Duration Density Functions (DDFs). The logarithmically-distributed histogram bins are represented by power functions (i.e., #days = coef * Q^{exp}) and scaled by the maximum daily flow of record. Given a way to predict the shape (exponent), magnitude (coefficient), and scale (Q_{max}) based on physical parameters, one could predict long-term durations of sediment-transporting flows for any ungauged watershed. More importantly regarding hydromodification, DDFs could simulate the increases in durations of sediment-transporting flows associated with unmitigated urbanization by including a statistically-significant surrogate measure (e.g., TIA) in the model. In this light, DDFs can become a central tool in understanding, modeling, and mitigating the effects of hydromodification in southern California.

Study Domain

Southern California is generally described in this study as the greater Los Angeles/San Diego area within about 100 mi of the Pacific coast, including portions of Ventura, Los Angeles, San Bernardino, Orange,

Riverside, and San Diego Counties and ca. 20 to 25 million residents. Mountain ranges to the north (Transverse Ranges) and east (Peninsular Ranges) offer fairly well-defined geologic bounds, with a total relief of up to 11,500 ft (3,500 m) and short travel distances to the ocean on the order of 50 mi (~80 km). The steep slopes promote runoff and produce more hydrologically-efficient watersheds than low-relief settings.

The climate is broadly characterized as Mediterranean, but precipitation and vegetative influences tend to increase with elevation, although there are obvious differences between the west (wetter) and east (drier) slopes of the Peninsular Ranges due to an effective 'rain shadow'. Regional extremes of average annual precipitation range 8 to 40 in/yr (200 to 1,000 mm/yr), while vegetation changes from sparse grasses and chaparral to dense coniferous stands at higher elevations. When rains do fall, they can be intense; the 2-yr 24-hr rainfall ranges ~2 to 6 in. (50 to 160 mm) across the domain.

This leads to a flashy regime with short-lived instantaneous peak flows that are much larger than the corresponding daily means. For example, a 10-yr instantaneous event would typically attenuate to a daily-mean flow on the order of a 2- to 3-yr event, with the former likely ten to twenty times the latter. Systems are predominantly ephemeral and clearly dominated by overland flow with little groundwater storage relative to humid systems. The heterogeneous lithologies have variable infiltration capacities, but differences seem to be overwhelmed during high-intensity storms, although they probably play a role in seepage losses during transmission (Knighton, 1998).

Beyond seasonal patterns, large fluctuations in annual, decadal, and even multi-decadal precipitation result in an active fire regime. Regional fires are often newsworthy for both direct (e.g., property destruction and mass evacuations) and indirect damage (e.g., post-fire landslides and flooding), and the corresponding pulses in both sediment and runoff (Booker *et al.*, 1993; California Forest Service (CaFS), 1951; Gabet and Dunne, 2003; Los Angeles County Flood Control District (LACFCD), 1959; McPhee, 1989). As early as 1947, the CaFS had recorded post-fire peaks two to thirty times as large as pre-fire peak flows for equivalent storms in their experimental forest, with influence decreasing with storm magnitude.

Finally, during field investigations of recently-developed suburban neighborhoods, we saw little evidence of stormwater retention/detention. Developed watersheds often had lined channels (i.e., concrete or riprap) and energy dissipaters at outfalls were occasionally present. Large regional basins and dammed reservoirs do exist; however, flow controls in watersheds less than ~40 mi² (~100 km²) were largely lacking. With the understanding that unmitigated urbanization largely increases flow variability, and that streams in southern California are inherently flashy, we hypothesize that the effects of urbanization may be especially pronounced.

Methods

Gauge data are made publicly available by the USGS, which adheres to strict quality assurance/quality control procedures prior to publishing flows as accepted/approved. To ensure comparable quality in processing and analysis, we developed the following methods. Some of the methods include a limited presentation and discussion of preliminary ‘results’ that informed model design and/or were less central to the overall conclusions of this research. For example, regarding peak flows, it was necessary to decide on a distribution prior to the building of statistical models. Gauge-selection criteria, below, describes how we tested several distributions and which was selected to use in model design.

The following sub-sections summarize the methodological process by which we arrived at final models and conclusions. First, we systematically-selected regional gauges and processed their peak-flow data. Next, we developed a method for processing and representing all daily-mean flows via cumulative histogram-based functions. Methods were then considered for objectively representing urbanization extent. Next, informed by literature and a theoretical understanding of surface-drainage network hydrology, an expansive array of spatially-based variables was populated for inclusion in the analyses. Lastly, analytical methods are presented including a cross-validation procedure that guided final model design.

Unit Disclaimer

Acknowledging the general preference of International System (SI) units among the scientific community, we felt it was beneficial to develop these equations in U.S. Customary System (or English) units for more direct comparisons to the U. S. Geological Survey (Waananen and Crippen, 1977) equations. Without becoming overly cumbersome, we try to offer SI units in parentheses and some figures are expressed in SI units.

Gauge-Selection Criteria

Our first step was the systematic selection of regional gauges for model development. The focus was on watersheds less than $\sim 100 \text{ mi}^2$ (250 km^2), primarily due to the fact that most of the region’s larger streams have been affected by dams and diversions. We excluded gauges that were artificially influenced by flow diversions to isolate only the effects of urbanization relative to the undeveloped, free-flowing setting.

We strove for a balance between a large representation of sites and gauges with sufficiently long records. Short records increase the likelihood of misrepresenting the true flow regime, while overly-conservative record-length requirements would eliminate the bulk of gauges. For example, only nineteen of the gauges within the study domain had records of 50 yrs or more; however, there were forty-nine gauges with records greater than 20 yrs. There was a natural break in the record lengths of the candidate gauges at ca. 15 yrs (two gauges at 18 yrs with one gauge at 14 yrs and the balance less than ca. 8 yrs). With limited urban/semi-urban gauges (i.e., only eight gauges $> 2.5\%$ imperviousness), the fact that the 14-yr record was in a partially urban watershed (imperviousness = 2.7% in 2001) supported its inclusion. This totaled fifty-two gauges with a spatial distribution depicted in Figure 1. A

summary of selected gradients such as drainage area and record length is provided in Table 1 (a comprehensive dataset may be obtained by contacting the corresponding author). These gradients also serve as bounds to the applicable ranges of our models.

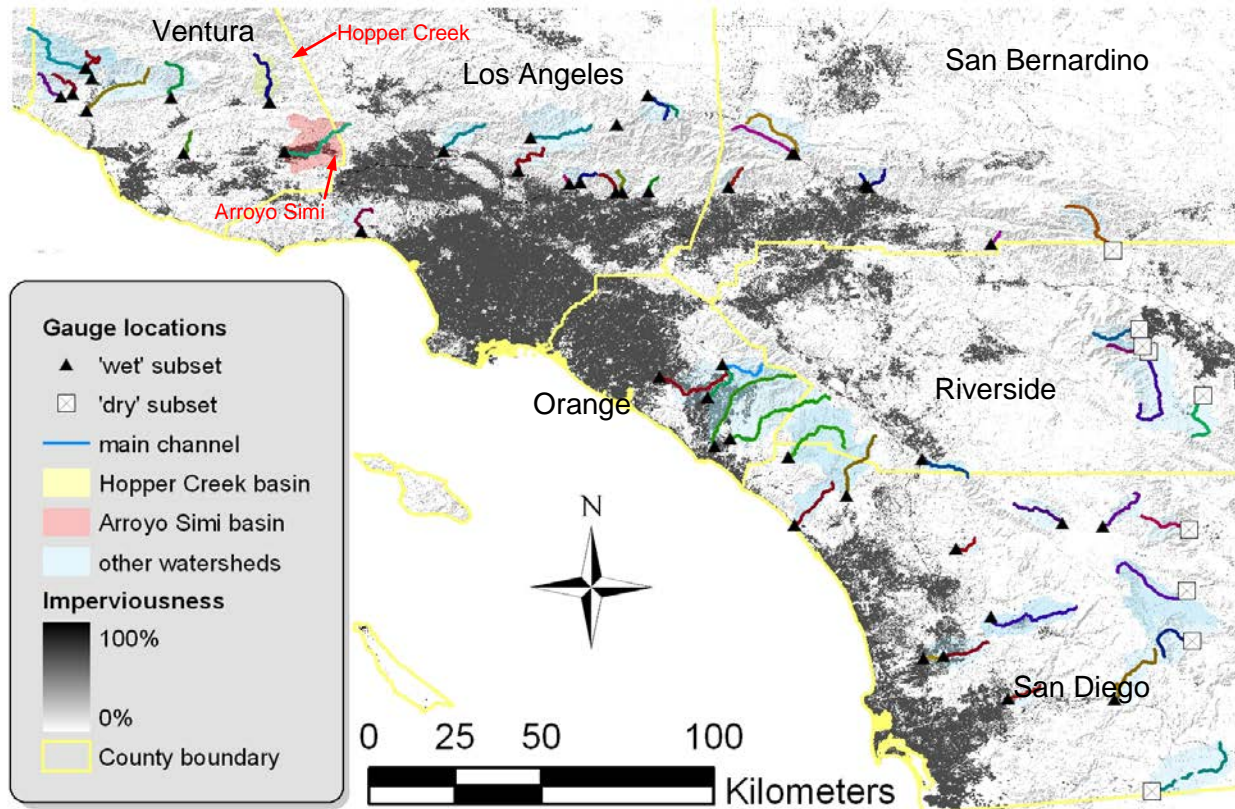


Figure 1. Locations of gauges used in equation development ('wet' subset) with corresponding watershed and main channel, overlaid by a gradient of imperviousness and county boundaries, with rural (Hopper) and urban (Arroyo Simi) case study gauges.

Table 1. Selected^(a,b) gradients of the forty-three USGS gauged watersheds used to develop models (i.e., model-application bounds), and the nine hydrogeomorphically-distinct gauges^(c) that were withheld from models.

Variable	USGS GAUGE IDENTIFICATION					FLOW RECORD			ROAD DENSITY		IMPERVIOUSNESS			PRECIPITATION		HYDROGEOMORPHIC					
	Name	Number	Latitude	Longitude	HUC8	Begin	End	Total ^(d)	2007	Avg ^(e)	2001	Max ^(e)	Avg ^(e)	Mean Annual ^(f)	2-yr 24-hr ^(g)	Drainage Area ^(h)	Drainage Density ⁽ⁱ⁾	Average Basin Elevation ^(j)	Average Channel Slope ^(k)	Average Surface Slope ^(k)	Valley Slope at Gauge ^(l)
Abbreviation	Gauge	No	Lat	Long	HUC 8	Begin	End	YrsPeak	Rdnsty07	RdnstyAv	Impv01	ImpMax	ImpAv	P	P224	DA	DD	ElvAvg	SlpChn	SlpSurf	SlpVly
Units	(decimal (decimal degrees) degrees)					(calendar (calendar yr) yrs)			(km/km ²) (km/km ²)					(mm)	(mm)	(km ²)	(km/km ²)	(m)			
Forty-three gauges included in model development	1	AGUACALIENTECNR WARNERSPRINGS	1103150033.2886	-116.653118070303	1961	1987	27	0.48	0.27	0.1%	0.1%	0.1%	434	64	49.5	1.26	1,184	4.0%	30%	0.8%	
	2	ALISOCAELTORO	1104750033.6261	-117.684218070301	1930	1980	50	6.80	1.83	20.3%	8.1%	1.4%	408	73	22.6	0.96	261	2.2%	18%	1.3%	
	3	ARROYOSECONRPASADENA	1109800034.2222	-118.176718070105	1910	2008	94	0.99	0.55	0.5%	0.5%	0.4%	803	131	41.7	1.79	833	4.6%	53%	3.3%	
	4	ARROYOSIMINRSIMI	1110585034.2731	-118.786918070103	1933	1983	50	4.08	1.97	10.0%	8.6%	4.9%	447	86	180.0	1.42	417	1.9%	23%	0.8%	
	5	ARROYOTRABUCOASAN JUANCAPISTRANO	1104730033.4983	-117.665018070301	1970	2008	23	5.35	3.95	18.8%	18.8%	14.2%	462	79	140.7	1.13	357	2.1%	25%	0.9%	
	6	BIGROCKCNRVALYERMO	1026350034.4208	-117.838618070106	1923	2008	84	0.67	0.36	0.4%	0.5%	0.4%	781	126	59.4	1.07	1,626	7.9%	50%	3.2%	
	7	BUCKHORNCNRVALYERMO	1026390034.3431	-117.920318090206	1960	1966	37	0.14	0.02	0.2%	0.2%	0.2%	889	150	1.4	1.22	2,228	20.2%	31%	21.1%	
	8	CAJONCNRKEENBROOK	1106300034.2669	-117.456418070203	1920	1982	58	1.86	0.85	1.4%	1.3%	0.8%	495	114	104.9	1.02	1,125	3.4%	25%	2.3%	
	9	COYOTECREEKNEAR OAKVIEW	1111760034.4167	-119.369718070101	1958	1988	30	0.51	0.31	0.0%	0.0%	0.0%	715	129	34.2	1.39	548	7.9%	39%	3.9%	
	10	CUCAMONGACNRUPLAND	1107347034.1794	-117.628118070203	1929	1975	48	0.23	0.01	0.0%	0.0%	0.0%	908	159	25.0	1.60	1,448	17.8%	59%	10.9%	
	11	DELUZCNRFALLBROOK	1104490033.3697	-117.321718070302	1951	2005	18	1.47	1.00	0.3%	0.3%	0.3%	529	60	122.8	1.18	242	2.0%	26%	0.1%	
	12	ETWINCNRRARROWHEAD SPRINGS	1105850034.1792	-117.264718070203	1919	2008	87	0.63	0.31	0.7%	0.7%	0.5%	848	129	22.6	1.73	954	11.6%	45%	5.2%	
	13	FISHCNRDUARTE	1108450034.1658	-117.923318070106	1916	1979	62	1.01	0.49	0.1%	0.1%	0.1%	840	130	16.5	1.71	701	9.7%	51%	2.2%	
	14	HONDABARRANCANRSOMIS	1110700034.2689	-119.048918070103	1954	1963	18	1.41	0.96	0.3%	0.3%	0.3%	468	76	6.1	2.15	233	3.9%	23%	2.4%	
	15	HOPPERCREEKNEARPIRU	1111050034.4008	-118.825618070102	1930	1983	49	0.53	0.04	0.0%	0.0%	0.0%	557	110	61.6	1.64	595	4.6%	42%	1.1%	
	16	KEYSCTRIBAVALLEYCENTER	1104020033.2292	-117.035818070303	1970	1991	14	3.71	2.70	2.7%	2.7%	2.5%	571	78	19.9	1.28	454	1.7%	8%	1.4%	
	17	LASFLORESCNROCEANSIDE	1104610033.2922	-117.455818070301	1951	2008	41	0.64	0.43	0.8%	0.9%	0.7%	383	54	68.2	1.63	134	1.6%	20%	0.7%	
	18	LITTLEDALTONCNR GLENDORA	1108650034.1675	-117.837518070106	1939	1971	33	1.61	1.06	0.1%	0.1%	0.1%	735	121	7.1	1.19	665	10.3%	48%	6.0%	
	19	LITTLESANGORGONIOCNR BEAUMONT	1105650034.0292	-116.945318070203	1948	1985	36	1.57	1.14	0.5%	0.5%	0.4%	801	120	4.6	1.55	1,736	16.8%	45%	8.6%	
	20	LITTLESANTAANITACNR SIERRAMADRE	1110050034.1869	-118.043118070105	1916	1979	46	0.72	0.03	0.1%	0.1%	0.1%	888	142	4.8	1.34	981	18.6%	56%	11.1%	
	21	LITTLETUJUNGACNRSAN FERNANDO	1109650034.2744	-118.371718070105	1928	1973	45	1.63	0.73	1.0%	0.8%	0.7%	581	98	53.7	2.56	641	4.6%	36%	1.7%	
	22	LONEPINECNRKEENBROOK	1106350034.2664	-117.463118070203	1920	2007	77	1.27	1.13	0.4%	0.4%	0.4%	568	136	39.3	1.31	1,357	6.6%	34%	4.4%	

Variable	USGS GAUGE IDENTIFICATION					FLOW RECORD			ROAD DENSITY		IMPERVIOUSNESS			PRECIPITATION		HYDROGEOMORPHIC							
	Name	Number	Latitude	Longitude	HUC8	Begin	End	Total ^(d)	2007	Avg ^(e)	2001	Max ^(e)	Avg ^(e)	Mean Annual ^(f)	2-yr 24-hr ^(g)	Drainage Area ^(h)	Drainage Density ⁽ⁱ⁾	Average Basin Elevation ^(j)	Average Channel Slope ^(k)	Average Surface Slope ^(l)	Valley Slope at Gauge ^(l)		
	Abbreviation	Gauge	No	Lat	Long	HUC 8	Begin	End	YrsPeak	Rdnsty07	RdnstyAv	Impv01	ImpMax	ImpAv	P	P224	DA	DD	ElvAvg	SlpChn	SlpSurf	SlpVly	
Units	(decimal(decimal degrees)degrees)					(calendar(calendar yr) yr) (yrs)	(km/km ²) (km/km ²)					(mm)	(mm)	(km ²)	(km/km ²)	(m)							
23	LOSCOCHE	SCNRLAKESIDE	11022200	32.8361	-116.8994	18070304	1983	2008	24	3.89	3.78	9.1%	9.1%	8.9%	366	58	31.7	1.13	288	2.5%	17%	1.6%	
24	LOSPENASQUITO	SCNR POWAY	11023340	32.9431	-117.1208	18070304	1964	2008	43	4.71	3.42	20.1%	20.1%	14.2%	353	53	108.9	1.23	287	2.6%	18%	1.3%	
25	LOSPENASQUITO	SCBL POWAY	11023330	32.9492	-117.0692	18070304	1969	1993	23	4.10	2.83	17.2%	15.2%	12.2%	361	54	80.9	1.21	319	3.6%	18%	0.8%	
26	NFMATIL	IJA	11116000	34.4925	-119.3056	18070101	1928	1983	50	0.44	0.15	0.1%	0.1%	0.1%	826	122	41.1	1.89	772	7.7%	44%	3.8%	
27	PECHANGAC	NRTEMECULA	11042631	33.4642	-117.1239	18070302	1987	2007	20	1.18	1.07	1.6%	1.6%	1.4%	448	66	34.7	1.31	605	4.8%	22%	0.8%	
28	ROGERS	SCNRAZUSA	11084000	34.1653	-117.9056	18070106	1917	1962	45	0.82	0.28	0.1%	0.1%	0.1%	815	125	17.3	1.59	526	6.2%	54%	3.6%	
29	SANANTONIO	CACASITAS SPRINGS	11117500	34.3803	-119.3036	18070101	1949	1983	34	2.76	1.74	1.2%	1.2%	1.1%	605	122	132.4	1.47	380	2.8%	30%	1.4%	
30	SANDIEGO	CATCULVERDRNR IRVINE	11048500	33.6817	-117.8086	18070204	1949	1985	36	4.90	2.01	23.4%	14.9%	6.4%	366	64	107.7	1.13	144	1.2%	11%	0.7%	
31	SANJUAN	NRSANJUAN CAPISTRANO	11046500	33.5189	-117.6242	18070301	1928	1969	41	0.97	0.37	2.3%	0.3%	0.3%	467	75	273.9	1.37	343	1.8%	28%	1.4%	
32	SANMATEO	CNRSAN CLEMENTE	11046300	33.4708	-117.4722	18070301	1952	2008	30	0.98	0.75	0.1%	0.1%	0.1%	515	70	209.5	1.13	404	2.2%	28%	0.7%	
33	SANTAANAC	NROAKVIEW	11117800	34.4236	-119.3403	18070101	1958	1988	30	0.93	0.69	0.1%	0.1%	0.1%	768	135	23.3	1.50	604	9.2%	41%	3.0%	
34	SANTAANITAC	NRSIERRA MADRE	11100000	34.1917	-118.0164	18070105	1916	1970	54	0.73	0.21	0.1%	0.1%	0.1%	889	143	25.1	1.54	944	14.1%	54%	8.1%	
35	SANTAMARIA	CNRRAMONA	11028500	33.0522	-116.9447	18070304	1912	2008	68	2.92	2.15	2.5%	2.5%	2.1%	496	64	147.3	1.00	574	1.5%	11%	0.4%	
36	SANTAPAU	LACNRSANTA PAULA	11113500	34.4133	-119.0814	18070102	1927	2007	72	0.87	0.53	0.1%	0.1%	0.1%	774	136	99.5	1.44	903	8.9%	40%	2.8%	
37	SANTIAGO	CAMODJESKA	11075800	33.7128	-117.6442	18070203	1961	2007	46	0.39	0.22	0.2%	0.2%	0.2%	596	93	33.7	1.26	683	5.1%	47%	1.7%	
38	SWEETWATER	NRNRDE SCANSO	11015000	32.8347	-116.6222	18070304	1905	2008	73	1.47	0.97	0.3%	0.3%	0.2%	697	105	117.3	1.22	1,223	1.9%	21%	2.0%	
39	TOPANGA	CNRTOPANGABCH	11104000	34.0644	-118.5861	18070104	1930	1979	49	3.47	2.26	1.4%	1.4%	1.1%	564	98	46.6	1.66	250	2.5%	30%	3.8%	
40	TUJUNGA	CBMILLCNRCOLBYRANCH	11094000	34.3092	-118.1444	18070105	1948	1971	24	0.64	0.30	0.2%	0.2%	0.2%	667	123	168.0	1.43	1,242	4.5%	37%	2.4%	
41	VENTURAR	NRMEINERSOAKS	11116550	34.4650	-119.2889	18070101	1959	1988	27	0.25	0.07	0.1%	0.1%	0.1%	856	132	192.1	1.91	774	4.3%	46%	1.1%	
42	WATERMAN	CANYON CREEKNR ARROWHEADSPRINGS	11058600	34.1858	-117.2722	18070203	1921	1985	65	2.40	1.54	1.5%	1.5%	1.1%	905	128	12.5	0.96	890	10.6%	45%	7.6%	
43	WFSANLUIS	REYRNR WARNERSPRINGS	11033000	33.2967	-116.7589	18070303	1913	1986	30	0.43	0.18	0.0%	0.0%	0.0%	780	98	66.0	1.15	1,164	4.3%	24%	1.5%	
with field	44	ANDREAS	CNRPALM SPRINGS	10259000	33.7600	-116.5492	18100200	1948	2008	59	0.00	0.00	0.0%	0.0%	0.0%	386	72	23.4	1.41	1,001	14.9%	51%	7.9%

Variable	USGS GAUGE IDENTIFICATION					FLOW RECORD			ROAD DENSITY		IMPERVIOUSNESS			PRECIPITATION		HYDROGEOMORPHIC					
	Name	Number	Latitude	Longitude	HUC8	Begin	End	Total ^(d)	2007	Avg ^(e)	2001	Max ^(e)	Avg ^(e)	Mean Annual ^(f)	2-yr 24-hr ^(g)	Drainage Area ^(h)	Drainage Density ⁽ⁱ⁾	Average Basin Elevation ^(j)	Average Channel Slope ^(k)	Average Surface Slope ^(l)	Valley Slope at Gauge ^(l)
Abbreviation	Gauge	No	Lat	Long	HUC 8	Begin	End	YrsPeak	Rdnsty07	RdnstyAv	Impv01	ImpMax	ImpAv	P	P224	DA	DD	ElvAvg	SlpChn	SlpSurf	SlpVly
Units	(decimal(degrees) decimal(degrees))					(calendar(yr) calendar(yr) yrs)	(km/km ²) (km/km ²)					(mm)	(mm)	(km ²)	(km/km ²)	(m)					
45	BORREGOPALMCNR BORREGOSPRINGS	10255810	33.2789	-116.4292	18100200	1950	2004	52	0.21	0.04	0.0%	0.0%	0.0%	317	48	56.4	1.36	1,043	7.5%	41%	12.7%
46	CAMPOCNR CAMPO	11012500	32.5911	-116.5247	18070305	1936	2008	71	1.47	1.09	0.5%	0.5%	0.4%	430	60	218.5	0.82	938	1.9%	12%	2.2%
47	DEEPCNR PALMDESERT	10259200	33.6311	-116.3914	18100200	1962	2008	46	0.58	0.43	0.7%	0.7%	0.6%	281	58	78.8	1.16	1,337	7.8%	30%	12.0%
48	MISSIONCNR DESERTHOT SPRINGS	10257600	34.0111	-116.6272	18100200	1967	2008	40	0.10	0.00	0.1%	0.1%	0.1%	519	99	91.8	1.51	1,475	7.0%	45%	4.4%
49	PALMCYN CNRPALM SPRINGS	10258500	33.7450	-116.5347	18100200	1930	2008	73	0.44	0.21	0.3%	0.3%	0.2%	297	57	241.3	1.63	932	4.2%	26%	2.2%
50	SANFELI PECNR JULIAN	10255700	33.1186	-116.4344	18100200	1958	1983	25	1.08	0.76	0.4%	0.3%	0.3%	445	65	230.8	1.46	864	1.8%	24%	4.8%
51	TAHQUITZ CNRPALM SPRINGS	10258000	33.8050	-116.5583	18100200	1947	2008	59	0.00	0.00	0.0%	0.0%	0.0%	562	92	44.1	1.43	1,563	15.0%	41%	6.4%
52	VALLECITO CNR JULIAN	10255850	32.9861	-116.4194	18100200	1963	1983	20	0.58	0.38	0.2%	0.2%	0.2%	400	67	102.4	1.58	988	5.0%	30%	2.2%
Gradients of the forty-three gauged watersheds used in model development (and model application bounds)					min	1905	1962	14	0.14	0.01	0.0%	0.0%	0.0%	353	53	1.4	0.96	134	1.2%	8%	0.1%
					mean	1940	1989	44	1.78	1.06	3.3%	2.7%	1.8%	633	103	71.1	1.41	745	6.2%	34%	3.3%
					max	1987	2008	94	6.80	3.95	23.4%	20.1%	14.2%	908	159	273.9	2.56	2,228	20.2%	59%	21.1%

^(a) Table includes all USGS gauges in the study domain with watersheds less than ~250 km², flow records greater than ~15 yrs, and no upstream dams/diversions.

^(b) Gaps in U.S. Department of Agriculture (USDA) geospatial soil coverages precluded the inclusion of soil characteristics in the analysis; however, a representative sample of regional watersheds ranged from 100% Natural Resources Conservation Service (NRCS) Type D to 100% NRCS Type B and up to 10% Type A soils with undeveloped NRCS Curve Numbers that ranged 77 to 88 with a mean of 83.4.

^(c) The nine gauges in Hydrologic Unit Code (HUC) 18100200 and 18070305 were excluded from model development due to their significantly (p < 0.05) different hydrogeomorphic setting on the east slope of the Peninsular Range.

^(d) Total years of annual maximum instantaneous peak records as recorded and made available by the USGS (i.e., not necessarily equal to "End" minus "Begin" due to intermittent records at several gauges).

^(e) Average and maximum road density and impervious values based on integration of spatial extent over the gauge records using three to four measures of spatial extent in time, delineated from historical USGS quadrangle maps and contemporary geospatial coverages from USGS and CalAtlas in a GIS.

^(f) Mean annual precipitation integrated over the watershed using USGS shapefile developed using regional precipitation data from 1900 to 1960.

^(g) Total precipitation volume over 24-hr duration with a probability of occurrence once every 2 yrs, spatially integrated over the watershed using NRCS shapefile developed using regional precipitation data from 1961 to 1990.

^(h) Contributing watershed area delineated in a GIS using the USGS HUC boundaries and a 10-m National Elevation Dataset (NED).

⁽ⁱ⁾ Drainage density developed using total stream length in basin as delineated in a GIS using the USGS National Hydrography Dataset (NHD) developed at a 1:24,000 scale.

^(j) Average basin elevation and channel slope measured after USGS protocol using points at 10 and 85% of the main-channel distance from gauge to basin divide.

^(k) Average surface slope of the entire watershed using clipped NED model from USGS.

^(l) Representative valley slope over reach at gauge I

The gauges had relatively-normal distributions of variables such as record length, precipitation, and surface slope, although drainage area and density showed a small positive skew. Imperviousness, however, had a highly-positive skew of 2.2. As of 2001, only fifteen gauges had watersheds with more than 1% TIA, while only six were greater than 10% imperviousness.

Another notable spatial trend was that eight gauges located in the eastern-most portion of the domain and one gauge in the far southeast at the Mexican border ('dry' subset Figure 1) lie in what is effectively a rain shadow. Stratified by USGS 8-digit Hydrologic Unit Codes (HUCs) of 18100200 or 18070305, the so-called 'dry' gauges were subject to less mean-annual precipitation as well as different types of events (i.e., local convective thunderstorms in addition to winter frontal storms). Hawley (2009) demonstrated significantly-different hydrologic behavior in the 'dry' subset, so much so that models were developed by using a discontinuous 'dummy' variable. In order to develop more targeted models for the balance of the gauges, we excluded the 'dry' subset in this study, making the final sample size forty-three and our models not applicable for watersheds east of the Peninsular Ranges (i.e., HUCs 18100200 and 18070305).

Instantaneous Peak Flows

Procedures were developed to populate recurrence-interval flows for the 1-, 1.5-, 2-, 5-, 10-, 25-, 50-, and 100-yr events from peak-flow data as recorded by the USGS. Their method seemed to be a hybrid of an annual-maximum and partial-duration approach, with an average of one record per calendar/water year, but cases of same-year peaks and occasional gaps during dry years. If a gauge was online during a no-flow year and a corresponding peak of 0 was not already recorded, the record was augmented to standardize the sample size at all gauges, populating an annual-maximum series. This was required on seven gauges and had clear implications on Q_1 ; however, it had little effect on higher recurrence intervals. For example, recurrence probabilities such as $Q_{1.5}$ and Q_2 generally had several similar flows near those rankings such that a shift would still result in a flow from the same range (e.g., 349 versus 331 cubic feet per second (cfs) for $Q_{1.5}$ and 570.5 versus 571 cfs for Q_2 at Arroyo Seco). Even less effect would be seen at the higher flows (i.e., $p = 1:25$ versus $1:24$ is effectively equivalent as representative of the 25-yr flow).

Other cases of record gaps included years with the date and/or stage of the peak but no flow. Interpolations based on USGS-rating relationships were used to estimate a reasonable flow for that date based on equivalent gauge heights and/or daily-mean flows. This was performed at eight gauges, representing less than 20% of the total. The interpolated flows were not used to determine a flow for a specific return interval; rather, they were simply used as placeholders in the plotting-position rankings.

Next, flows were proportionally ranked to determine recurrence probabilities via the Weibull plotting position (Chow, 1964; Yevjevich, 1972). Several commonly-used probability distributions were then tested to represent the flow-frequency relationship at each gauge, including the normal, lognormal (LN), exponential, and gamma. Because a central component of this paper is an updated alternative to the USGS 1977 regional equations, we also considered the Log-Pearson Type III (LP3), a log-transformed three-parameter gamma distribution that has been the standard USGS flow-frequency method since

1967 (U. S. Water Resources Council, 1967). Distributions were fit by minimizing residual squares between recorded and modeled flows (i.e., method of moments) giving proportional weight to the larger flows; whereas, the reverse procedure would dampen the significance of larger flows by minimizing residuals among recurrence probabilities. With easily-invertible distributions (e.g., normal, LN, and gamma) we fit flows directly to recurrence probabilities, whereas distributions that could not be solved analytically when inverted required alternative solutions (e.g., weighted skew factor (G) for the LP3 method).

Despite application in previous studies, the LP3 performed relatively poorly due to the flashy regimes and the corresponding effect on the skew factor. Even by following the recommended weighting scheme (U. S. Water Resources Council, 1981), the large number of gauges with years of very low or no flow typically converted a highly-positive skew in arithmetic space to a negative skew after the log-transformation. As discussed by Chow *et al.* (1988), this imposes an artificial upper bound on the data. Attempts to account for the low/zero flows within the confines of the LP3 method via the addition of correction factors both large ($\log(Q + 100 \text{ cfs})$) and small ($\log(Q + 0.1 \text{ cfs})$) were regularly outperformed by a simple regression of flow (Q_i) as a function of log-transformed recurrence interval $\{\ln(i)\}$ (Figure 2).

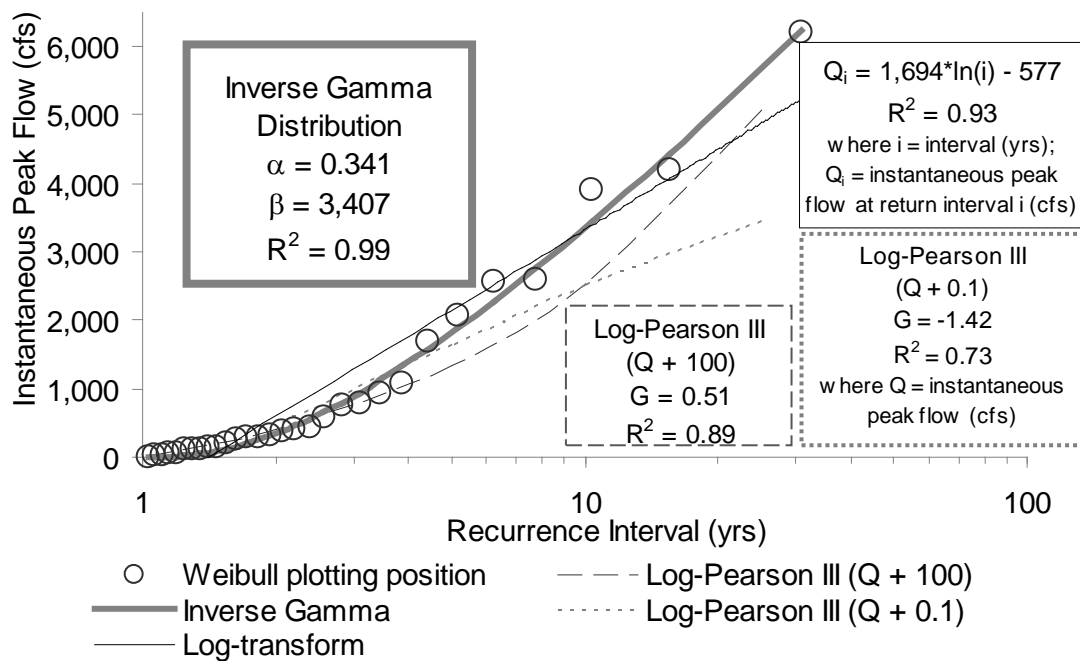


Figure 2. Flow versus recurrence interval of 30-yr record at USGS gauge no. 11033000, West Fork San Luis Rey River near Warner Springs, California, with Log-Pearson Type III adjusted (Q + 0.1) and (Q + 100) and inverse gamma distributions, and log-transform function.

Among all tested distributions, the inverse gamma with parameters α and β was superior in every case in terms of homoscedasticity of residuals and R^2 (e.g., mean and median R^2 0.95 and 0.97, respectively, with only three cases < 0.90). Bounded by zero by definition, the gamma function is ideal for modeling skewed distributions without the need for a log transformation (Chow *et al.*, 1988) – befitting for the flashy ephemeral regimes of southern California. Gamma-distribution flows were used to develop models for flows greater than or equal to the 5-yr interval, while the Weibull plotting position was used for the 1-, 1.5-, and 2-yr events due to nominal interpolation gaps over the smaller ranges given the relatively-large record lengths.

Long-Term Cumulative Durations

Although peak flows are important in understanding erosive energy at a given return interval, flow durations offer a much more complete understanding of the cumulative sediment-transport potential. Accordingly, we developed procedures to mathematically represent all daily-mean flows on record with cumulative duration curves. First, daily-mean flows were binned via a histogram procedure analogous to the initial steps of an effective-discharge calculation after Biedenharn *et al.* (2000, 2001). Histogram bins were scaled by the maximum daily-mean flow on record (Q_{\max}) rather than an instantaneous peak flow (e.g., Q_2 after Watson *et al.* (1997)) for two reasons. First, as described in detail later, Q_{\max} values could be predicted with much greater accuracies than the highly variable Q_2 . Second, scaling with Q_{\max} ensured consistent temporal scales for the duration analyses because daily-mean discharges were the only long-term records widely available (i.e., opposed to shorter intervals such as 1 hr or 15 min) and the two time scales were not transferable or even scalable. That is, the ratio of peak to daily mean was not consistent across return periods, sites, or even equivalent flows at the same site. For example, two equivalent 10-yr peak flows recorded at the same gauge could have corresponding daily-mean flows that differed by a factor of two in rural settings, and up to three in urban settings, potentially attributable to the spatial extent, intensity, or even timing of the event.

Regarding the selection of the type and number of bins for our models, the truly limiting factor in sediment-distribution curves – the ultimate application of our models – is ensuring a relatively-continuous flow-frequency distribution such that no bins are populated by 0 days of occurrence (Biedenharn *et al.*, 2000, 2001). Although arithmetic bins are statistically more prudent, the extreme flashiness of ephemeral streams in southern California made logarithmic bins the only practical way to represent flow frequency without discontinuities. The following equation was used to size logarithmically-equivalent bins after Raff *et al.* (2004):

$$H_{B-\log} = \{\ln (Q_{\max}) - \ln (Q_{\min})\} / (N_B - 1) \quad \text{Eq. (1)}$$

where:

- $H_{B-\log}$ = bin size of logarithmically-spaced histogram bins;
- Q_{\max} = maximum flow of record;
- Q_{\min} = minimum flow of record; and
- N_B = number of bins.

For consistency across all gauges toward development of a regional equation, we set Q_{\min} equal to 0.01 cfs at all sites, the lowest non-zero daily-mean flow reported by any gauge. Bins 1 through N_B were then populated by the total number of days of occurrence at flow rates within the respective bins. Lower and upper bounds of each logarithmically-spaced bin were determined using the following equations after Raff *et al.* (2004):

$$B_{\text{lwr-log}} = e^{\{\ln(Q_{\min}) + (B-2) * H_{B-\log}\}} \quad \text{Eq. (2)}$$

$$B_{\text{upr-log}} = e^{\{\ln(Q_{\min}) + (B-1) * H_{B-\log}\}} \quad \text{Eq. (3)}$$

where:

- $B_{\text{lwr-log}}$ = lower logarithmically-spaced bound of bin number (B);
- $B_{\text{upr-log}}$ = upper logarithmically-spaced bound of bin number (B); and
- B = bin number (i.e., 1 to N_B , where N_B = total number of bins).

Setting N_B equal to 25 provided a reasonable balance of resolution (small bin sizes) and continuous frequency distributions. All but three gauges, Buckhorn (6 yrs), Honda Barranca (9 yrs), and Keys C (14 yrs), had daily-flow records long enough to sufficiently populate 25 bins. Little San Gorgonio, despite having a long enough record (37 yrs), was skewed by an extreme flow resulting in 3 of the top 6 bins being empty with the remaining three only having 1 day of occurrence. An additional three gauges (Cucamonga, Pechanga, and Waterman) each had 1 bin populated with 0 days of occurrence, but because the adjacent bins were amply populated, we could ‘borrow’ 0.5 days from each adjacent bin to convert the 0-day bin into a 1-day bin. Of the original forty-three gauges, this resulted in thirty-nine that could be included in the DDF models.

In order to represent the histograms in a concise, transferable format, the next step was to convert them into *conditional* Probability Density Functions (PDFs) by fitting power functions to the centroids of the bins representing the geomorphically-effective range of flows. Again looking toward application, with a high likelihood of under-predicting sediment transport due to data intervals of days rather than minutes (Watson *et al.*, 1997), further bias was avoided by fitting the DDFs to the arithmetic-bin centroids, as opposed to the logarithmic centroids. This positioned each centroid on a slightly higher flow than the otherwise geometric centroid (e.g., 806 cfs versus 774 cfs for bin 21 at San Antonio, or 8,119 cfs versus 7,793 cfs for bin 25). Given that sediment transport increases non-linearly with flow, such a scheme would better approximate the composite transport of the individual flows within the bin.

The next consideration was which bins would be important to represent for sediment transport. Their distributions were relatively continuous over bins 12-25, and particularly continuous over bins 16-25, such that they could be well-represented with simple power functions. Fortuitously, those bins that could be well-fit coincided with the same ranges that would be important for sediment transport. From preliminary analyses it was apparent that streams characterized by threshold behavior (i.e., bankfull dimensionless shear stress (τ_{*BF}) \sim 0.03 to 0.06) would be sufficiently represented with a 16-25 scheme,

while live-bed channels (i.e., $\tau_{*BF} \sim 1$ to 10+) would require the broader range. As demonstrated by Hawley (2009), cumulative sediment transport became relatively insignificant below bin 12, despite cases of entrainment at lower flows.

Figure 3 offers an example of a typical DDF fit of bins 16-25 at the San Antonio gauge. Overlaid in Figure 3 is the De Luz gauge as an example of one of the poorer fits (i.e., eight gauges with $R^2 < 0.95$, three gauges < 0.90). By depicting two gauges with relatively similar watersheds, Figure 3 also alludes to the significance of the gauge-record length. DDFs scaled nonlinearly with years of duration, primarily attributable to the extreme flashiness and inter-year variability in precipitation. Longer gauge records have higher probabilities of experiencing an extreme precipitation event, corresponding to nonlinear increases in flows and durations.

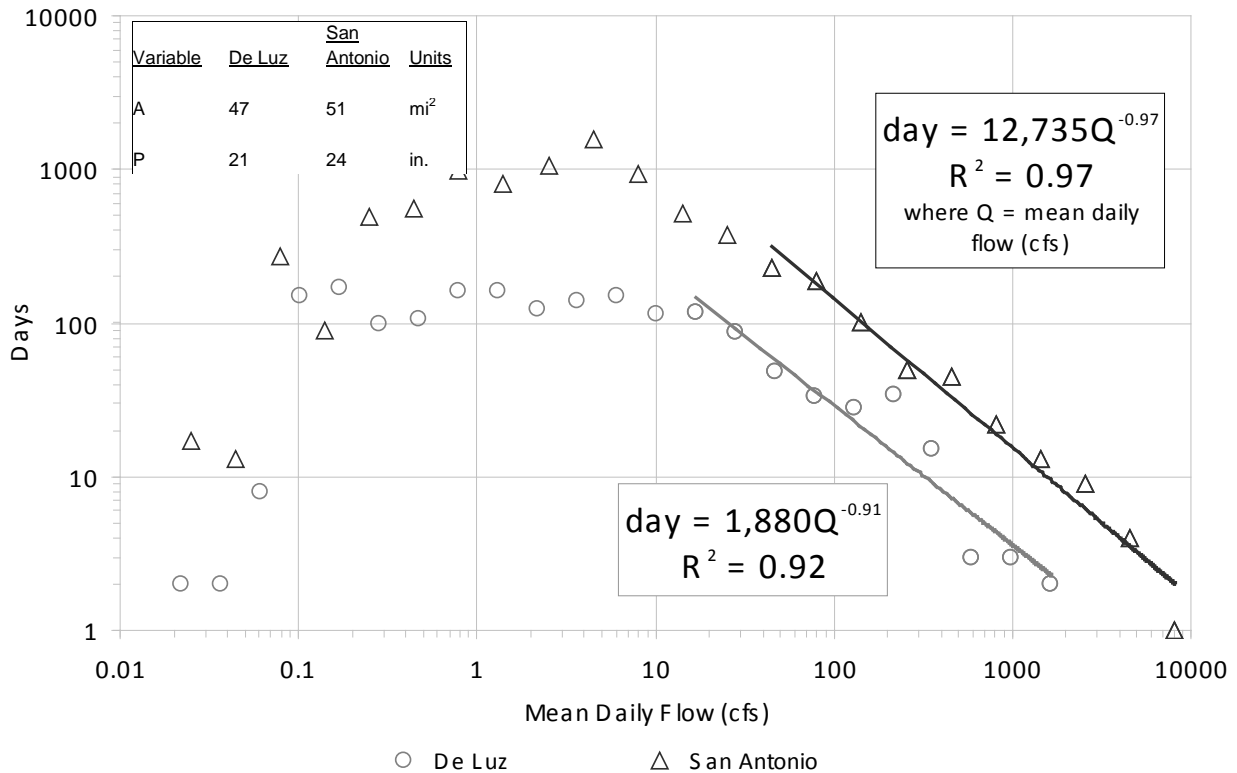


Figure 3. DDFs of gauges De Luz and San Antonio fitted to centroids of logarithmically distributed histogram bins 16-25 with selected variables of drainage area (A), average annual precipitation (P), and record length (Yr).

The 16-25 scheme with the coefficient and exponent parameters termed d1 and d2, respectively, showed largely-homoscedastic residuals (Figure 3) at the risk of not capturing all sediment-transporting bins in live-bed channels (bin 16 of San Antonio = 45 cfs). The second scheme, termed day1 and day2, regressed bins 12-25 to more conservatively include all significant sediment-transporting flows (e.g., bin 12 at San Antonio = 4.5 cfs). However, as one could envision with De Luz (Figure 3), the disadvantage in

including bins 12-15 is that it resulted in more heteroscedastic residuals at some gauges. R^2 values were also slightly worse, with eleven gauges less than 0.95 and five gauges less than 0.90. The general form of the power functions used in the respective schemes is:

$$\text{days}_{@Q} = d1 * Q^{d2} \quad (\text{bins 16-25, i.e., } \tau_{*BF} \sim 0.03 \text{ to } 0.06) \quad \text{Eq. (4)}$$

$$\text{days}_{@Q} = \text{day1} * Q^{\text{day2}} \quad (\text{bins 12-25, i.e., } \tau_{*BF} \sim 1 \text{ to } 10+) \quad \text{Eq. (5)}$$

where:

- days_{@Q} = number of days of occurrence at flow rate (Q);
- Q = arithmetic average of daily-mean flows corresponding to the lower- and upper-bin boundaries defined by Eqs. (2) and (3), respectively (cfs);
- d1 = coefficient for power function fit to bins 16-25;
- d2 = exponent for power function fit to bins 16-25;
- day1 = coefficient for power function fit to bins 12-25;
- day2 = exponent for power function fit to bins 12-25; and
- τ_{*BF} = dimensionless shear-stress ranges at approximate 'bankfull' flow range (i.e., on the order of Q_{10}) corresponding to threshold (0.03 to 0.06), and live-bed (1 to 10+) behavior.

With the outlined methods for processing daily-mean flows, DDFs were fit to all gauges to populate a matrix of their respective components (i.e., Q_{max} , d1/day1, d2/day2). The dataset was used to develop models of each DDF component as multivariate functions of statistically-significant watershed descriptors, offering an objective method for estimating flows and cumulative durations at ungauged locations.

Measures of Urbanization

An investigation focused on understanding the influence of urbanization on flow regimes should dedicate great care to measuring its extent. With the goal of objectively representing urbanization in both space and time, we first looked to what other researchers have used to characterize it, including but not limited to:

- % impervious area (Booth, 1991, 2000; Espey and Winslow, 1974; Galster *et al.*, 2006; Leopold, 1968; Sauer *et al.*, 1983),
- % developed (Galster *et al.*, 2006; Rantz, 1971),
- % served by storm sewers (Leopold, 1968; Rantz, 1971),
- % paved (Hollis, 1975),
- road density (Konrad and Booth, 2002),
- population density (Konrad and Booth, 2002; Sauer *et al.*, 1983), and

- numerical indices, e.g., function of channel conditions, stormwater connectivity, etc. (Espey and Winslow, 1974; Sauer *et al.*, 1983).

Measures have ranged from qualitative groupings (e.g., rural versus urban) to fully-continuous variables (e.g., % impervious). One of the more widely used approaches is to employ the USGS National Urban Equations developed by Sauer *et al.* (1983). The second most significant variable in the seven-parameter approach is the Basin Development Factor (BDF), which is a somewhat subjectively-assigned composite index (0 to 12) of channel improvements, channel linings, storm drains/sewers, and curb and guttered streets.

We had several goals regarding the quantification of urbanization in our equations. First, despite being an empirical approach, assurance of fidelity to hydrologic processes was desired. Next, measures should be readily quantifiable via publically-available GIS data (i.e., no subjectivity or field investigations necessary). Third, the variable should be a continuous metric wherever possible (e.g., % impervious) rather than taking the form of a categorical variable such as high, medium, and low. Finally, because urbanization is not constant through time, we needed to be able to measure changes in spatial extent over the gauge records.

Arguably, the measure of urbanization that is most rooted in theory and most important hydrologically is imperviousness (Novotny, 2003). Impervious surfaces diminish infiltration potential, eliminate interception storage of plant surfaces, and decrease surface roughness relative to soil/vegetated surfaces, all of which acts to increase direct surface runoff and the rate at which it flows. However, it is whether an impervious surface is *connected* to the drainage network that determines if the potential effects are transferred downstream. Effective Impervious Area (EIA) is defined as impervious surfaces that are directly connected to the downstream drainage system, consequently excluding any areas draining to pervious surfaces (Booth and Jackson, 1997). Although it is more representative of process than TIA, EIA can be arduous to measure. The two metrics have been correlated on regional scales such as for Denver, Colorado (Alley and Veenhuis, 1983), and western Washington (Dinicola, 1989); however, large differences in stormwater regulations throughout the country both in space and time suggest that the application of such relations to other regions would be imprudent. Fortunately for this research (although unfortunately for receiving streams), stormwater at the subdivision scale in southern California has largely gone unmitigated to date. This makes TIA generally much more representative of EIA than in other regions. Additionally, TIA is readily quantifiable in GIS via the USGS national impervious raster from 2001, meeting both criteria of being objectively quantifiable and largely representative of process.

Other important physical descriptors of urbanization are alterations of the hydrologic network via storm sewers, channelization/lining, or artificial surface storage. The latter has a diminishing effect on peak flows, while the other network adjustments can amplify peaks via decreased roughness and often shorter/steeper flow paths. Unfortunately, no public domain GIS layers were available to quantify storm sewers; therefore, it was decided to measure both road density and impervious area as potential surrogates. The USGS National Hydrography Dataset (NHD) offered measures of known artificial-channel adjustments in existing stream networks (e.g., 'artificial path', 'canalditch', 'connector', or

'pipeline'). Quantifications of such artificial stream-network links were included, although they did not prove to be statistically significant in preliminary models.

As such, impervious area and road density were used as the primary measures of urbanization. State of California (Cal-Atlas) road vectors from 2000 and 2007, along with a USGS impervious raster (2001), provided contemporary measures. The 2000 vector file was clipped to match georeferenced historical USGS topographic quadrangle maps, providing two additional snapshots of road density in time (typically ranging between the 1950s to 1980s). An example at one of the most urban gauges, Arroyo Trabuco (gauge no. 11047300), is presented in Figure 4, along with 2001 impervious levels. Knowing which roads were not constructed at respective points in time provided the basis for clipping-out associated impervious areas from the 2001 raster file such that changes in imperviousness through time could also be estimated. This procedure was performed for each watershed greater than 1% impervious area in 2001 (15 gauges), with the expectation that watersheds with less than 1% impervious area in 2001 would show little change in development through time. As a check to see how urban measures changed in a rural setting, the historical procedure was performed on one gauge with 0.4% impervious area in 2001 (Lone Pine, gauge no. 11063500).

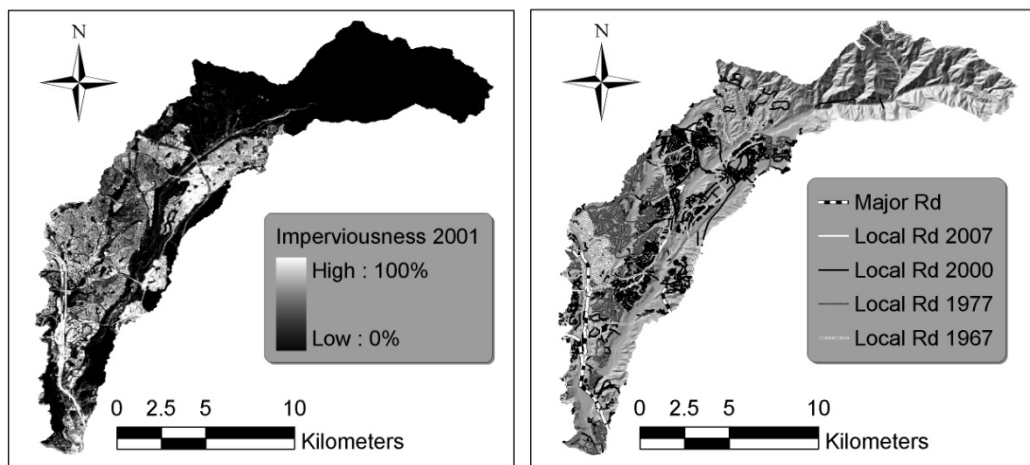


Figure 4. 2001 imperviousness and road vectors tracked through time per USGS historic quadrangle maps and current Cal-Atlas shapefiles at Arroyo Trabuco (Orange County, California, near intersection of Interstates 5 and 405).

It was apparent from the historical analysis that both road density and imperviousness tended to progress relatively linearly during development phases (Figure 5) such that the trapezoidal rule was sufficient to integrate mean values over the record. The gauges with the five highest integrated road densities (i.e., > 4 mi/mi²) were covered by measured values of road density over their entire flow record. However, it was necessary to develop procedures to estimate measures of urbanization at gauges with records extending beyond the earliest measured values (e.g., pre-1950s). Given that the

earliest measured values indicated relatively undeveloped/rural settings, Hawley (2009) was able to converge on a consistent procedure for all gauges where extrapolations were required.

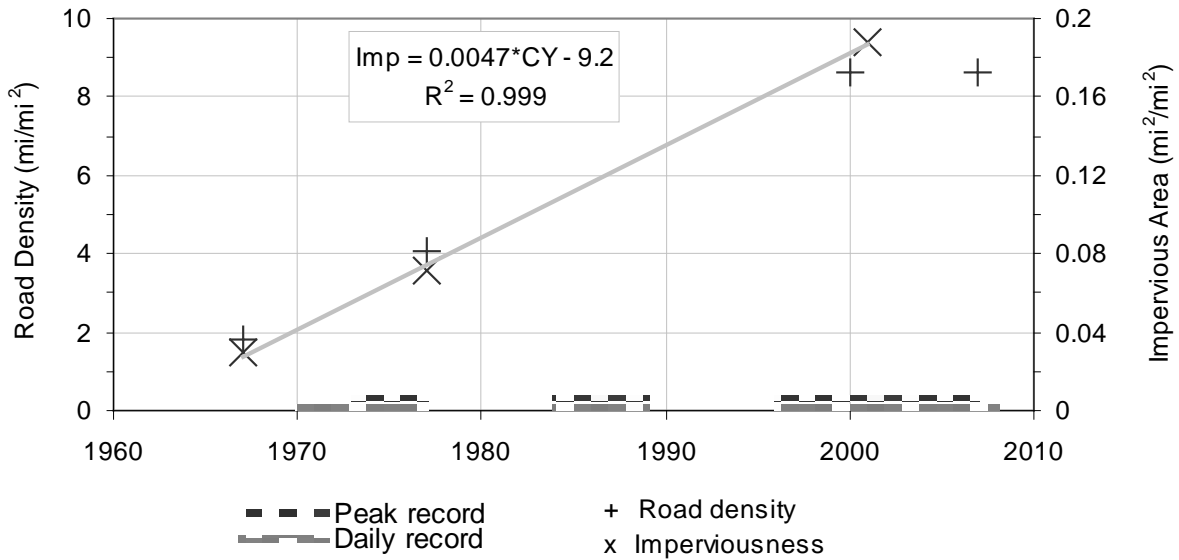


Figure 5. Imperviousness and road density through time at Arroyo Trabuco, overlaid by active gauge years and linear regression of imperviousness (Imp) as a function of calendar year (CY) from 1967 to 2001.

After tracking the progression of urbanization in great detail, several time-integrated measures were quantified of both road density and impervious area for testing in the models. Those that proved to be most consistently significant (i.e., $p < 0.05$) in preliminary models are indicated in **bold**:

- Imperviousness (TIA)
 - **Average spatial extent** (i.e., aerial extent of total imperviousness tracked through time and integrated over gauge record)
 - **Maximum spatial extent** (i.e., aerial extent of total imperviousness during last year of gauge record)
 - Fraction of record > (i.e., amount of time out of total years of record greater than xx% impervious area)
 - 1.5%
 - **5%**
 - **7.5%**
 - 10%
 - 15%

- Road Density
 - Average spatial extent
 - Maximum spatial extent
 - Fraction of record >
 - 2 mi/mi²
 - 4 mi/mi²
 - 5 mi/mi²
 - 6 mi/mi²
 - 8 mi/mi²

One potential explanation for the discrepancy in statistical significance between impervious area and road density is that TIA is a better surrogate for EIA than road density given such little stormwater mitigation to date. Furthermore, although the road density and imperviousness tend to be linearly correlated (e.g., Figure 5) at individual sites, they are *exponentially* correlated across all sites. As evident in Figure 6, a relatively-undeveloped gauge in a rural setting could have road densities up to 4 mi/mi² and still have minimal amounts of impervious area (i.e., ~1.5%), while a gauge in a developing watershed with just 50% higher road density could have over seven times as much impervious area (i.e., 6 mi/mi² relative to 10% imperviousness). This exponential relation masks potentially-critical differences in imperviousness in the early phases of development when ~2 mi/mi² could represent less than 0.1% TIA in a rural basin or greater than 2% in a developing basin. The correlation is also misrepresentative in highly urbanized basins, as the relationship seems more linear than exponential above ~6 mi/mi². Such a complex, discontinuous relationship between road density and TIA would make it difficult for a continuous model to use one measure as a surrogate for the other.

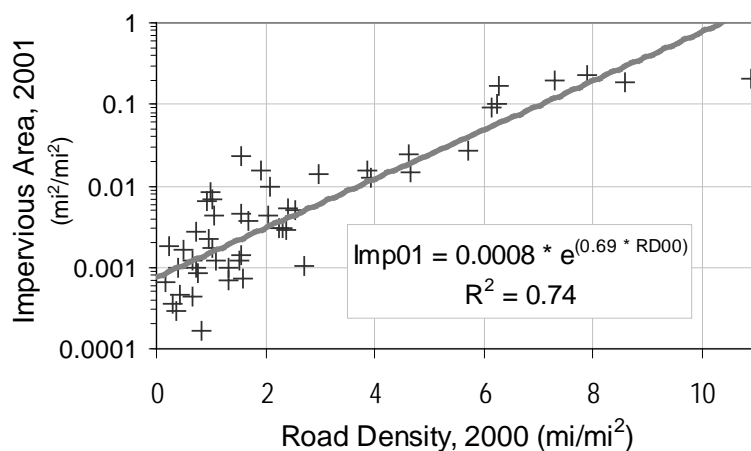


Figure 6. Exponential correlation between impervious area in 2001 (Imp01) and road density in 2000 (RD00) across all sites.

Other Physically-Based Metrics

One way to avoid specious conclusions in empirical studies is to develop multiple competing hypotheses (Schumm, 1991). It is not enough to infer causation by observing higher flows in urban settings. To be truly exhaustive, alternatives should be offered such as: were the urban gauges set in steeper watersheds, were they active during exceptional precipitation years, etc.? A matrix of readily-quantifiable hydrogeomorphic metrics was populated across varying temporal and spatial scales (Table 2) to test the influence of a multitude of potentially competing factors. GIS data (see Reference section) were acquired from public-domain sources such as the USGS, U.S. Department of Agriculture (USDA), National Oceanic and Atmospheric Administration (NOAA), and State of California geospatial clearinghouse (Cal-Atlas). Empty fields in some USDA polygons precluded a complete analysis of Natural Resources Conservation Service (NRCS) soil types; however, most source data were complete. Two sources of average annual precipitation were available. The USGS layer (1900 - 1960) was of slightly coarser spatial grain than the NRCS (1961 - 1990) shapefile, but because the 1977 USGS equations for southern California were developed with the former, both precipitation coverages were tested in the models. General resolution of these data was such that their precision was typically on the order of 1% of the measurement (e.g., 10-m National Elevation Dataset (NED) over 1 km of channel).

Table 1. Summary of variables tested in models with corresponding significance.

	Variable ^(a)	Units	Definition (equation)	GIS Source/Scale
spatial (x and y)	A	mi ²	drainage area	HUC and NED/10m
	Stm	mi	total stream length	NHD/ 1:24,000
	DD	mi/mi ²	drainage density (DD = Stm/A)	
	L	mi	length of main channel from gauge to basin divide	
	Shp	mi/mi ²	main-channel length divided by drainage area, i.e., shape (Shp = L/A)	
	W _{vy}	ft	valley width, measured from base of hillslope at gauge location	
	Ord	-	order – Strahler (1952) stream order	
	Arf _{Stm}	-	artificial fraction of total stream length, i.e., code ≠ 460	NHD
	Arf _{Mn}	-	artificial fraction of main channel	
	Rlf	ft	total relief along main channel (elevation at divide minus elevation at gauge)	
topographic (x, y, and z)	Elev	ft	average basin elevation, i.e., average of elevations at 10% and 85% of main-channel length measured from gauge to divide	
	Gage	ft	elevation at gauge	
	S _{chn}	ft/mi	average slope of main channel via elevations at 10% and 85% points	
	V _{ly}	ft/mi	valley slope at gauge measured across geomorphically-continuous valley ~10% of main-channel length or ~1,500 ft (500 m)	
	S _{rf}	ft/ft	average surface slope of watershed	

	Variable ^(a)	Units	Definition (equation)	GIS Source/Scale
precipitation	P	in.	average annual precipitation (area-weighted)	USGS (1900 - 1960)
	<i>Pnr_{cs}</i>	in.	average annual precipitation (area-weighted)	NRCS (1961 - 1990)
	P224	in.	2-yr 24-hr precipitation volume (area-weighted)	NRCS
	<i>IP</i>	-	precipitation intensity relative to annual average ($IP = P224/Pnr_{cs}$)	
	<i>LA_{hst}</i>	-	relative difference from long-term precipitation average of 15.07 in. recorded at LA during gauged years	(1878 - 2006)
	<i>LA_{w_tyr}</i>	-	number of exceptionally 'wet' precipitation years (50% > LA average, i.e., > 22.6 in.) during gauge record	
	<i>LA_{w_tt}</i>	-	relative number of exceptionally 'wet' precipitation years (50% > LA average) during gauge record divided by gauge record	
	<i>SD_{hst}</i>	-	relative difference from long-term precipitation average of 9.96 in. recorded at SD during gauged years	(1850 - 2005)
	<i>SD_{w_tyr}</i>	-	number of exceptionally 'wet' precipitation years (50% > SD average, i.e., > 14.9 in.) during gauge record	
	<i>SD_{w_tt}</i>	-	relative number of exceptionally 'wet' precipitation years (50% > SD average) during gauge record divided by gauge record	

^(a) Variables: primary in **bold**, secondary in *italics*, and no statistical significance is plain text

ArcMap software by Environmental Systems Research Institute (ESRI), including extensions such as 'spatial analyst', was used to optimize GIS measurements such as delineating watersheds and flow paths. Automated results from NED processing were cross-checked with existing shapefiles such as USGS HUC boundaries and NHD flowlines to verify estimates of drainage area, drainage density, etc.

Figure 7 depicts the inter-annual, decadal, and multi-decadal trends in regional precipitation as recorded at the two long-term precipitation gauges in Los Angeles (LA) and San Diego (SD). It includes the number of active gauges as well as number of gauges above specified levels of road density, suggesting that the more urban period of record (post ~1970) potentially had larger volumes of precipitation than the pre-urban period. By looking at records of individual gauges, Figure 8 shows some of the more urban records were active during wetter years; however, the most urban gauge (Arroyo Trabuco) was active during one of the driest composite climates on record. As such, we included the relative difference between mean-annual precipitation during flow records, along with the number of exceptionally wet years (50% > mean), in the models.

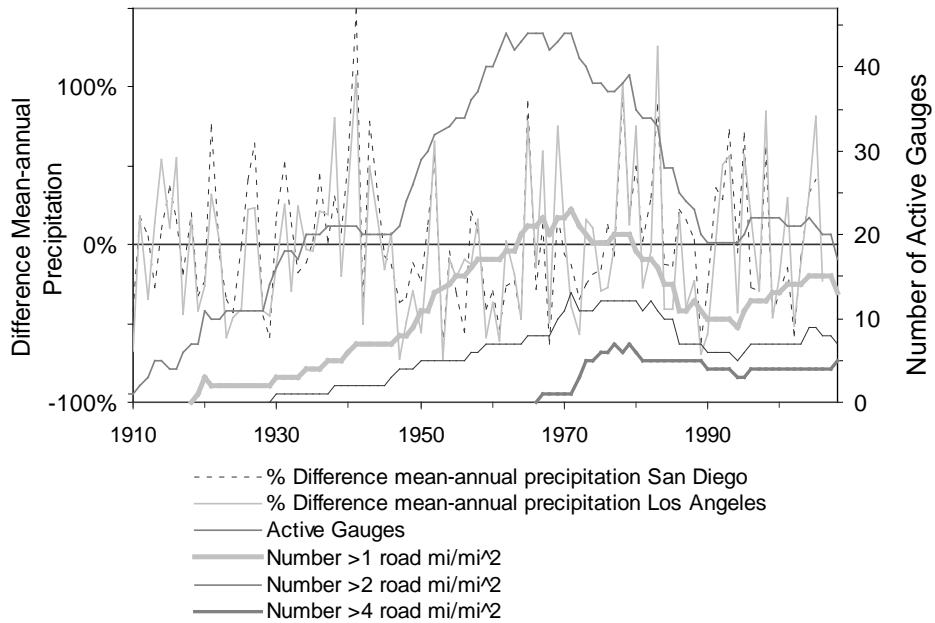


Figure 7. Inter-annual precipitation variability recorded at Los Angeles and San Diego overlaid with number of active gauges and number of gauged watersheds exceeding specified road-density levels (indicating increasing urbanization).

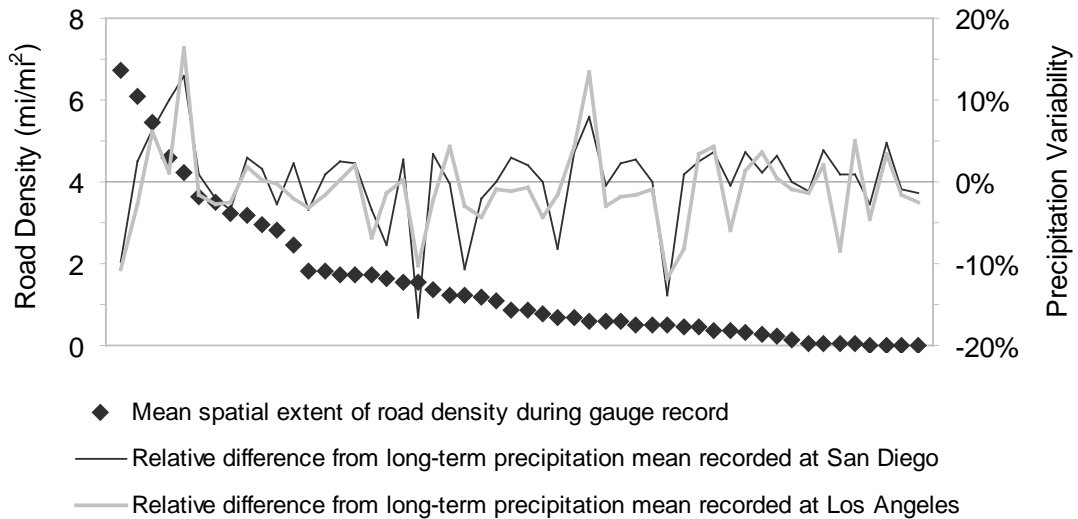


Figure 8. Mean spatial extent of road density overlaid by relative difference from long-term mean-annual precipitation recorded at Los Angeles and San Diego during gauge records.

Watershed configurations and drainage patterns varied throughout the study domain from linear to circular and parallel to dendritic, respectively. The slight departure in the overall trend of main-channel length (length of longest stem from gauge traced to drainage divide) as a function of drainage area from Hack's (1957) relationship is less notable than the variance within the sample (Figure 9), particularly important because one of the most exceptionally-linear watersheds (Arroyo Trabuco, 37 km to 140 km²) was also one of the most urbanized. To represent these potentially-significant differences, the parameter 'Shp' was added as an alternative independent variable, defined as main-channel length/area.

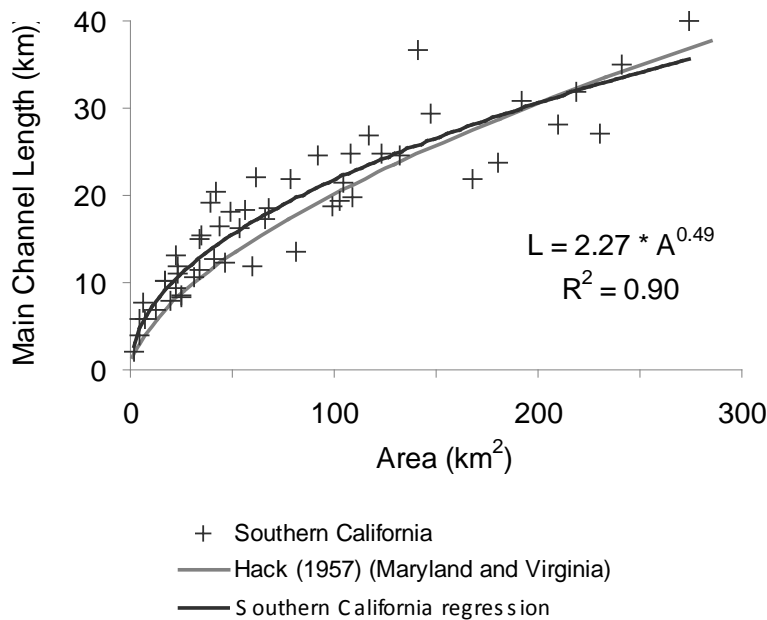


Figure 9. Main-channel length to basin divide (L) versus drainage area (A): southern California and the Hack (1957) relationship from Maryland and Virginia.

Consistent with Gregory (1976), drainage density was positively correlated to mean-annual precipitation in the semiarid regime and negatively correlated in the more humid setting (Figure 10). Additional parameters not explicitly accounted for in the models were vegetative cover, soil type/depth, and bedrock permeability due to incomplete spatial data; however, vegetation density may be implicitly captured in a discontinuous/threshold manner via mean-annual precipitation – one of the process-based explanations to the pattern in Figure 10. Other potentially contributing, but admittedly inter-correlated, factors which exhibited similarly-shaped patterns with drainage density included the 2-yr 24-hr precipitation, average surface slope, and average basin elevation. Two additional variables that showed scattered, slightly-positive correlations with drainage density were total basin relief and the 2-yr 24-hr precipitation volume standardized by the mean-annual precipitation.

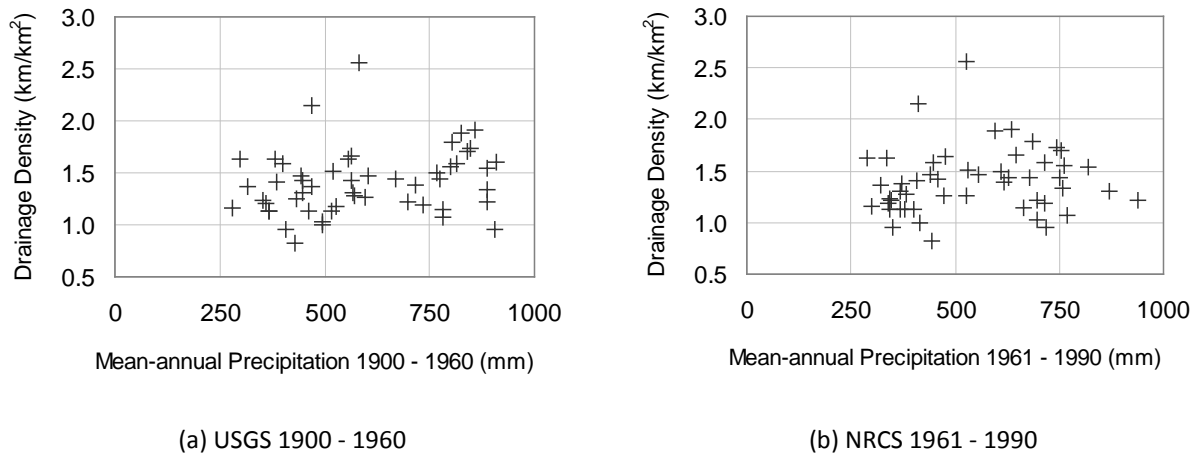


Figure 10. Drainage density versus area-averaged mean-annual precipitation.

Analytical Methods and Model Design

Beyond representing physical processes with appropriate quantitative variables, it was also important to guide their combination in model design to obviate potential collinearity issues. The objectives of the modeling were 2-fold: 1) to represent process by determining which variables were most significant in predicting flow magnitudes and durations, and 2) to determine which combinations and forms of these critical variables resulted in the most optimally-fit models for application. To guide the selection process, a cross-validation step was performed prior to final model design in which every fourth gauge (sorted alphabetically) was withheld resulting in a 33/10 calibration/validation split.

Multivariate power functions via regression analysis have been widely used by the USGS in developing regional equations for recurrence-interval flows (Jennings *et al.*, 1994). Logarithmic transformations of primary variables (e.g., Q, A, and P) in the southern California dataset created relatively constant residual variance, such that our analyses continue in this tradition. We used Statistical Analysis Software (SAS) to perform ordinary least squares regression. Hundreds of iterations of models were run with various withholding schemes using forward, backward, and best subset selection to determine the most consistently-significant parameters and candidate models for final testing. Due to sample variance, some variables were tested in multiple forms (e.g., exponential and power) and varied units (e.g., slope in ft/ft or ft/mi), expanding the range of variables from which the models could select.

Because unguided model selection often resulted in collinear variables and/or multiple forms of the same variable, our basic model framework was to test combinations of up to one variable from distinct process-based categories to preclude collinear variables from competing to represent the same process within the same model. Regarding peak-flow equations, the models selected from the following categories:

- watershed/network size: drainage area (A) or total stream length (Stm);
- spatial efficiency: shape (Shp) or drainage density (DD);
- precipitation: mean annual (P), 2-yr 24-hr volume (P_{224}), or 2-yr 24-hr relative to mean annual (IP);
- topographic efficiency: average slope of watershed surface (Srf), average channel slope (S_{chn}), valley slope at site (Vly), and total relief along main channel (Rlf);
- imperviousness (TIA): average imperviousness over record (Imp_{av}), maximum imperviousness of record (Imp_{max}), fraction of record length greater than 5% impervious (Imp_5), and fraction of record length greater than 7.5% impervious (Imp_7).

Identical steps were taken in designing equations for the component variables of DDFs (i.e., Q_{max} , d1/day1, and d2/day2). Beyond the process-based categories discussed above, a probabilistic category was added with candidate variables that increased the likelihood of having an extremely large/long event. This included the number of years of gauge record (Yr), the relative difference from long-term precipitation average recorded at LA during gauged years (LA_{hst}), and the number of active gauge years that were exceptionally 'wet', that is, 50% greater than the long-term mean recorded at LA ($LAwt_{yr}$ and $LAwt_{rt}$).

Finally, due to the fact that DDFs essentially pivot around Q_{max} , it was clear that their shape (i.e., d2 or day2) would best be explained by direct measures of their magnitude (d1 or day1) and scale (Q_{max}). All else being equal, a larger DDF magnitude would correspond to a steeper (more negative) slope, while a larger scale (Q_{max}) would tend to correspond to a flatter (less negative) curve. As such, d1/day1 and Q_{max} were included in some of the d2/day2 models to evaluate the performance benefits relative to the risk of compounding prediction errors on the application side. Instantaneous peak flows were also tested as a substitute for daily Q_{max} , with Q_{10} being the best candidate for final models due to performance in predicting d2/day2, as well as regularly having the best prediction accuracies among all instantaneous Q_i in preliminary models.

Model forms that were congruent with hydrologic theory and had high performance in the cross-validation phase were selected for final model calibration. Model performance was measured via several indicators such as a high significance of individual variables (typically $p < 0.05$), high Adjusted R^2 (Adj. R^2) and/or minimum corrected Akaike Information Criterion (AIC_c), and homoscedastic residuals across both calibration and validation data. We assessed model performance, including standard diagnostics, in both logarithmic and arithmetic space. Outliers were identified using standard diagnostics (e.g., Cook'D, Rstudent residual, etc.); however, to be withheld from the model there needs to be supporting *a priori* evidence and/or compelling physically-based justification (e.g., the hydrogeomorphically-distinct 'dry' subset of gauges east of the Penninsular Range discussed above). In general, we attempted to follow the guideline of ca. 10 observations per predictor variable, such that models from the cross-validation phase typically had only three to four independent variables (i.e., per thirty-three samples) allowing for exceptions in cases of high performance/statistical significance.

Results

The presentation of results is divided into three subsections: 1) cross-validation summary, 2) peak-flow equations, and 3) DDF models. Because competing models often performed similarly, we include five to six models for each dependent variable. This reduces the risk of giving too much weight to one model/variable as they are all physically based, and there is generally no clear basis for choosing one model over a similarly performing alternative. It also better represents the range of influence of urbanization in that different proportions of the variance are explained depending on what other statistically-significant variables are included.

Cross-Validation Summaries and Individual Variable Performance

Cross-validation models of Q_i and DDF components are summarized in Tables 3(a) and 3(b), respectively. Measures of watershed size (Stm, A) and precipitation (P, P_{224}) accounted for the most variance across all return-interval flows. Measures of imperviousness accounted for up to one quarter of the variance of the 1-yr flow, with decreasing significance for higher flows (e.g., partial $R^2 \sim 0.10, 0.06, 0.02$ for 1.5-, 2-, and 5-yr flows, respectively). At higher return intervals (i.e., $\geq Q_{10}$), the size of the watershed accounted for so much of the variance that few additional terms were statistically significant (i.e., $p < 0.05$), resulting in high performance using relatively-simple models. For example, for return intervals 10, 25, 50, and 100, R^2 in arithmetic space ranged from 0.7 to 0.9 for both calibration and validation subsamples using the following equations:

$$Q_i = f(A, P)$$

$$Q_i = f(\text{Stm}, P)$$

$$Q_i = f(\text{Stm}, P_{224}) \text{ (see Figure 11 for cross-validation performance at } Q_{25}\text{)}$$

Table 2. Summary of cross-validated models.

(a) For instantaneous peak flows ($n_{\text{calibration}} = 33, n_{\text{validation}} = 10$)

Dependent Variable	Urbanization Significant ($p < 0.05$) in Validated Model?	Best Predictor Variables ^(a)	Average Calibration Standard Error ^(b)	Average Validation Standard Error ^(b)
Q1.5	✓	A, Strm (0.2); P, P_{224} , IP, (0.2); Imp_{max} (0.1)	80%	100%
Q2	✓	A, Strm (0.4); P, P_{224} , IP (0.1); Imp_{max} (0.06)	80%	80%
Q5	✓	A, Strm (0.7); P, P_{224} , IP (0.1); Imp_{max} (0.02)	60%	70%
Q10	$p = 0.12$	A, Strm (0.8); P, P_{224} , IP (0.05)	40%	50%
Q25		A, Strm, (0.8); P, P_{224} , IP (0.07)	30%	50%
Q50		A, Strm (0.8); P, P_{224} , (0.08)	30%	50%
Q100		A, Strm (0.7); P, P_{224} (0.1)	40%	60%

Table 3. Continued

(b) For DDFs

Dependent Variable	n Calibration	n Validation	Urbanization Significant (p < 0.05) in Validated Model?	Best Predictor Variables ^(a)	Average Calibration R ^{2(c)}	Average Validation R ^{2(c)}
Qmax	33	10		A, Strm (0.6); P, P ₂₂₄ (0.2)	0.8	0.8
d1	29	9	✓	A (0.1); P (0.2); Yr (0.5); Imp _x (0.05)	0.7	0.9
day1	30	9	✓	A (0.1); P (0.2); Yr (0.5); Imp _x (0.1)	0.7	0.7
d2	30	9	p = 0.06	Q ₁₀ (0.3); d1 (0.5)	0.9	0.9
day2	30	9	✓	Q ₁₀ (0.3); day1 (0.5)	0.9	0.8

^(a) Corresponding partial R² in parentheses

^(b) Standard Error of estimate reported from arithmetic space as a percentage of the sample mean

^(c) R² reported from arithmetic space

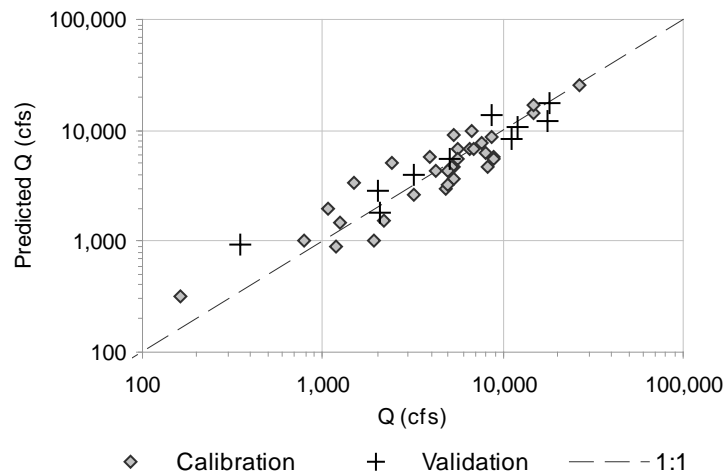


Figure 11. Cross-validation performance of $Q_i = f(\text{Stm}, P_{224})$ for 25-yr return interval (predicted Q_{25} versus actual) with 1:1 'perfect-fit' line overlaid.

However, the diminishing predictive power of watershed scale (i.e., A and Stm) with storm frequency (e.g., partial R² for A ~0.7 at Q₅ versus ~0.2 at Q_{1.5}) explained why equations with more classes of hydrologic variables generally performed better than simpler models for return intervals less than 5 yrs. That is, with decreasing volumes of precipitation, the efficiency with which a drainage network concentrated and conveyed runoff became increasingly significant in predicting peak flow. Although hundreds of models were tested, the form that performed best during cross validation in terms of arithmetic space R², AIC, SE, and least patterned residuals for Q_{1.5} and Q₂ was:

$$Q_i = f(\text{Stm}, \text{Shp}, \text{IP}, \text{Vly}, \text{Imp}_{\text{max}})$$

Imperviousness could account for up to 25% of variability in the 1-yr flow, but other terms had little predictive power. Largely attributable to the fact that fifteen of the forty-three gauges had entire years of no flow (i.e., $Q_1 = 0$), models showed poor overall performance and unacceptably-patterned residuals. Consequently, no Q_1 equations were advanced to final calibration.

Based on performance across all remaining return intervals (i.e., 1.5, 2, 5, 10, 25, 50, and 100), five base-models were selected for final calibration. A summary of the cross-validated models is presented in Table 3(a).

Recall that DDFs have three components: Q_{max} (scale), d1 or day1 (magnitude), and d2 or day2 (shape). Process-based categories such as scale and precipitation explained most of the variance of Q_{max} (partial R^2 of 0.6 and 0.2, respectively). Record length (Yr) was the next most significant variable in forward selection, explaining 3 to 4% of the variance. The most significant measure of network spatial efficiency was DD (2 to 3% of the variance) when used in combination with A, P or P_{224} , and Yr. Other measures of spatial and topographical efficiency were insignificant ($p \gg 0.05$) except in models where precipitation was intentionally withheld, which resulted in poorer overall performance. This suggested that the measures were acting more as a surrogate for precipitation. Finally, urbanization was insignificant in predicting the maximum daily-mean flow on record, consistent with the models of the rarest and largest peak flows (i.e., $\geq Q_{25}$).

Forward selection of DDF magnitude parameters typically identified the following form, with corresponding partial R^2 in parentheses:

d1: Yrs (0.52), A (0.05 - 0.06), P (0.14), Imp_x (0.04 - 0.06)

day1: Yrs (0.46), A (0.07 - 0.09), P (0.18), Imp_x (0.10 - 0.11), S_{chn} (0.02 - 0.03)

One of three similarly performing impervious descriptors (i.e., Imp_x representing Imp_{av} , Imp_5 , or Imp_7) was typically the third variable added during forward selection for 'day1', while it was generally the fourth best explanatory variable for 'd1'. Exponential forms of the impervious terms consistently explained more variance than the power form.

Models of day1 with S_{chn} had improved calibration accuracy but reduced validation performance compared to the base model (i.e., A, P, Yrs, and Imp_x). Adding both Srf (0.03 - 0.04) and DD (0.02 - 0.03) to the base model improved both calibration and validation performance. Despite reservations about including six independent variables with only thirty calibration observations, the fact that all variables were significant ($p < 0.05$) supported their inclusion. One model of d1 had modest performance with no urban term (A, DD, Srf, Yrs) during calibration, but had substandard performance with the validation data across all measures (i.e., R^2 , Adj. R^2 , SE, AIC, and AIC_c). It was selected for final model calibration in order to compare performance of urban models against the best non-urban model.

A substantial outlier was identified during the calibration/validation phase of d1. In this case, there was significant *a priori* rationale to consider excluding the Ventura River gauge near Meiners Oaks, California (gauge no. 11116550), because the DDF itself was poorly fit (worst R^2 at 0.79) with unacceptably-patterned residuals. Withholding the outlier resulted in substantial changes to the parameter values,

increased the significance of urbanization and drainage area (partial R^2 of 0.04 to 0.07 and 0.12, respectively), and improved overall model performance. Similar to the expanded day1 models, d1 as a function of A, P, DD, Srf, Yrs, and Imp_x resulted in improved performance in the validation data and less heteroscedastic residuals.

The shape of the DDFs (d2 or day2) was highly influenced by its magnitude (Q_{max}) and scale (d1 or day1). Models that intentionally withheld such measures were not only poorly fit (best Adj. R^2 0.57 for d2), but had severely patterned residuals. Conversely, models that included d1 (partial R^2 0.54) and Q_{max} (partial R^2 0.28), or Q_{10} (partial R^2 0.32) as an alternative to Q_{max} , accounted for up to 90% of the total variance. Inclusion of these variables was necessary to achieve high model performance ($R^2 > 0.6$).

Another significant outlier (Little Dalton near Glendora, California) was identified during d2 cross validation; however, there was no concurring *a priori* evidence to withhold the gauge from the models. Two similarly performing models were identified during calibration in the following forms:

$$d2 = f(Q_{10}, d1, Yrs, Imp_x)$$

$$d2 = f(Q_{10}, d1, Yrs, P_x)$$

The model with P or P_{224} in place of Imp_x performed slightly better during calibration (Adj. R^2 0.90 versus 0.88); however, had larger errors and more patterned residuals in validation (R^2 0.83 versus 0.93, Standard Error (SE) 14% versus 9%). Both were selected for final calibration, along with a three-term equation that substituted Slp_{chn} for Yrs and P, which performed slightly worse in both calibration and validation, but all terms were significant at the $p < 0.05$ level.

Likewise with the calibration of day2, Q_{10} and day1 explained most of the variance (0.31 and 0.51, respectively), with Q_{max} explaining 26% of the variance in the place of Q_{10} . Models that intentionally excluded those variables could barely explain the total variance that 'day1' could explain individually. Standard diagnostics revealed unacceptably-patterned residuals when plotted against Q_{10} . The shape, which slightly resembled the trend of drainage density versus precipitation (Figure 10), became less pronounced when Imp_x was included in the model. They were most evenly distributed by including P_{224} , Yr, and Elev in place of imperviousness, but the five-variable model for day2 performed the poorest with the validation data (R^2 0.56 versus 0.86 for $day2 = f(day1, Q_{10}, Yrs, Imp_{av})$). This was despite the fact that each variable in the five-variable model was significant at the 0.05 level during calibration and the model on the whole accounted for more variance (i.e., 91% versus 85%). As such, both models were selected for final calibration.

In summary, for each dependent variable, cross validation produced five to twelve reasonably performing candidate models that were advanced to final calibration; the best performing models are presented herein. A central finding was that measures of imperviousness were highly significant ($p < 0.05$) in predicting instantaneous peak flows at return intervals less than or equal to 5 yrs. Additionally, urbanization was highly significant in predicting the magnitude of DDFs ($p < 0.05$ in nineteen of twenty models, $p < 0.001$ in nine of twenty models). This was particularly true for the day1 (partial $R^2 \sim 0.10$) scheme that includes more bins with low/moderate flows (bins 12-25) as opposed to the d1 (partial R^2

~0.05) scheme which is more skewed toward the highest flows (bins 16-25). DDF shape (d2 or day2) was less explained by urbanization ($\rho < 0.10$ in four of fourteen models), other than through the indirect influence of DDF magnitude, which explained greater than 50% of the variance of its shape.

Peak-Flow Equations

Five equations are presented for each return-interval flows. By using the same equation formats for all recurrence intervals, it is apparent how the most influential variables change with return period. In general, there seems to be a behavior change around the 2- and 5-yr events, transitioning from a high influence of drainage efficiency, rainfall intensity, and imperviousness to a greater dependency on watershed size such as area and total stream length.

The equations have varied forms; however, the final equation (Eq. (10)) is intentionally presented as a revision to the USGS 1977 equations that were functions of only A and P. We added an exponential term for Imp_{max} because it models the effects of urbanization in a simple continuous form (i.e., $\text{Imp}_{\text{max}} \rightarrow 0$, urban term $\rightarrow 1$, equation \rightarrow rural equation). We present each equation with the corresponding variable definitions (in Table 2); and parameters, units, and performance measures (in Tables 4(a) through 4(j)) for each return interval. ***In these equations, uppercase terms indicate variables and lowercase nomenclature indicates the corresponding β parameter from the regression. Bold font draws attention to terms with varied units.***

Equation (6) is presented with corresponding parameters, units, and performance measures in Table 4(a):

$$Q_i = e^{(\text{Incpt})} * \text{Stm}^{\text{stm}} * e^{(\text{shp} * \text{Shp})} * \text{IP}^{\text{ip}} * \text{Vly}^{\text{vly}} * e^{(\text{impmax} * \text{Impmax})} \quad \text{Eq. (6)}$$

where:

- Q_i = instantaneous peak flow at return interval i yrs (cfs);
- Stm = total stream length in basin (mi);
- Shp = length of main channel (traced to basin divide) divided by total drainage area (mi/mi^2);
- IP = P_{224}/P_{nrCS} , i.e., 2-yr 24-hr volume/average annual volume: NRCS 1961 - 1990 (in/in);
- Vly = valley slope at gauge as measured across a geomorphically-continuous valley setting (i.e., relatively continuous valley width lacking major tributary confluences) up to a length of ~10% of main-channel length or ~1,500 ft (ft/mi); and
- Imp_{max} impervious area as **fraction** of total drainage area (mi^2/mi^2).

Table 3. Corresponding parameters, units, and performance measures for equations.

(a) For Eq. (6)

Return Period (yrs)	Incpt (-)	stm (mi)	shp (mi/mi ²)	ip (-)	vly (ft/mi)	imp _{max} (-)	Adjusted	Standard	AIC _c ^(c)	p-exceptions
							R ² ^(a)	Error ^(b)		(p > 0.05)
1.5	8.19	0.286	-1.03	3.49	0.448	9.21	0.53	68%	445	stm 0.32
2	7.99	0.376	-0.891	2.87	0.337	6.68	0.61	62%	487	stm 0.12, shp 0.07
5	8.86	0.647	-0.380	2.57	0.099	2.54	0.80	49%	591	shp 0.25, vly 0.37, imp _{max} 0.11
10	7.83	0.717	-0.344	1.77	0.137	0	0.86	39%	628	shp 0.19, vly 0.10
25	7.08	0.783	-0.282	1.31	0.197	0	0.84	39%	680	shp 0.31
50	6.82	0.811	-0.255	1.12	0.223	0	0.82	42%	714	shp 0.40
100	6.68	0.831	-0.236	0.99	0.241	0	0.80	45%	742	lp 0.10, shp 0.46

(b) For Eq. (7)

Return Period (yrs)	Incpt (-)	a (mi ²)	dd (mi/mi ²)	p224 (in.)	imp _{max} (%)	Adjusted	Standard	AIC _c ^(c)	p-exceptions
						R ² ^(a)	Error ^(b)		(p > 0.05)
1.5	-0.799	0.630	1.36	1.80	0.763	0.46	94%	471	dd 0.07
2	0.411	0.694	1.14	1.48	0.579	0.55	82%	508	dd 0.07
5	2.83	0.840	0.957	0.713	0.240	0.74	59%	604	imp _{max} 0.05
10	3.61	0.865	0.804	0.778	0.096	0.84	41%	633	imp _{max} 0.29
25	4.22	0.884	0.701	0.825	0	0.85	32%	659	
50	4.41	0.891	0.699	0.910	0	0.85	31%	687	
100	4.56	0.897	0.699	0.968	0	0.84	32%	712	

(c) For Eq. (8)

Return Period (yrs)	Incpt (-)	stm (mi)	p224 (in.)	imp _{max} (-)	Adjusted	Standard	AIC _c ^(c)	p-exceptions
					R ² ^(a)	Error ^(b)		(p > 0.05)
1.5	-0.188	0.628	1.81	13.1	0.48	83%	459	
2	0.837	0.689	1.46	9.91	0.56	74%	499	
5	3.00	0.835	0.678	3.99	0.74	56%	599	imp _{max} 0.05
10	3.62	0.859	0.748	1.70	0.84	40%	629	imp _{max} 0.26
25	4.16	0.876	0.781	0	0.86	32%	660	
50	4.34	0.884	0.864	0	0.85	31%	686	
100	4.50	0.889	0.921	0	0.84	33%	712	

Table 4. Continued

(d) For Eq. (9)

Return Period (yrs)	Incpt (-)	a (mi ²)	p ₂₂₄ (in.)	elv (ft)	imp _{max} (-)	Adjusted	Standard	AIC _c ^(c)	p-exceptions
						R ² ^(a)	Error ^(b)		(p > 0.05)
1.5	6.08	0.586	3.07	-0.960	10.8	0.57	67%	442	
2	6.99	0.656	2.71	-0.939	7.59	0.68	63%	486	
5	8.22	0.821	1.54	-0.733	0	0.80	47%	584	
10	7.45	0.850	1.55	-0.546	0	0.88	34%	615	
25	7.06	0.870	1.57	-0.426	0	0.87	32%	662	
50	6.95	0.879	1.58	-0.375	0	0.86	34%	695	
100	6.90	0.886	1.59	-0.340	0	0.84	37%	724	

(e) For Eq. (10)

Return Period (yrs)	Incpt (-)	a (mi ²)	p (in.)	imp _{max} (-)	Adjusted	Standard	AIC _c ^(c)	p-exceptions
					R ² ^(a)	Error ^(b)		(p > 0.05)
1.5	-2.03	0.592	1.55	11.6	0.37	85%	461	
2	-0.644	0.667	1.29	8.61	0.47	76%	501	
5	2.137	0.838	0.773	3.23	0.70	59%	603	P 0.08, Imp _{max} 0.17
10	2.90	0.868	0.767	0	0.81	45%	637	
25	2.68	0.891	1.01	0	0.83	37%	673	
50	2.63	0.902	1.11	0	0.82	37%	700	
100	2.62	0.909	1.19	0	0.81	38%	724	

(f) For Q_{max} (scale) equations for DDFs Eqs. (11) through (13)

Eq. Number	Incpt (-)	a (mi ²)	stm (mi)	yr (yrs)	dd (mi/mi ²)	p (in.)	p ₂₂₄ (in.)	Adjusted	Standard	AIC _c ^(c)	p-exceptions
								R ² ^(a)	Error ^(b)		(p > 0.05)
11	-2.24	0.979	-	0.341	-	1.79	-	0.80	51%	632	
11	1.44	0.966	-	0.288	-	-	1.65	0.81	49%	629	Yr 0.10
12	-2.35	0.974	-	0.362	0.687	1.63	-	0.81	48%	629	DD 0.10
12	1.06	0.960	-	0.315	0.624	-	1.50	0.81	46%	625	DD 0.13, Yr 0.07
13	-2.30	-	0.958	0.381	-	1.54	-	0.82	48%	628	
13	0.900	-	0.942	0.341	-	-	1.40	0.82	45%	623	

Table 4. Continued
(g) For d1 Eqs. (14) and (15)

Impervious-											
ness								Adjusted	Standard	p-values	
Variable	Incpt	a	p	yr	dd	srf	imp _x	R ² (a)	Error (b)	AIC _c (c)	for Imp _x
	(-)	(mi ²)	(in.)	(yrs)	(mi/mi ²)	(-)	(-)				
Imp _{av}	-15.6	0.891	4.89	1.65	-	-	10.2	0.81	173%	830	0.016
Imp ₅	-16.2	0.920	5.01	1.70	-	-	1.42	0.82	170%	829	0.005
Imp ₇	-16.8	0.945	5.13	1.74	-	-	1.82	0.84	167%	827	< 0.001
Imp _{av}	-12.9	1.07	3.74	1.64	-1.39	4.43	9.15	0.84	131%	813	0.020
Imp ₅	-13.6	1.09	3.90	1.69	-1.38	4.23	1.28	0.85	128%	811	0.006
Imp ₇	-14.2	1.11	4.05	1.73	-1.37	4.18	1.69	0.87	123%	808	< 0.001

(h) For d2 Eqs. (16) and (17)

Impervious-											
ness or Precipitation							Adjusted	Standard	p-values for		
Variable	Incpt	β _{Q10}	β _{d1}	β _{yr}	β _{Px}	β _{imp_x}	R ² (d)	Error (b)	AIC _c (c)	Imp _x or P _x	
	(-)	(cfs)	(days, cfs)	(yrs)	(in.)	(-)					
Imp _{av}	-1.91	0.193	-0.128	0.123	-	1.02	0.89	8.1%	-187	0.011	
Imp ₅	-1.95	0.195	-0.130	0.130	-	0.124	0.89	8.1%	-186	0.012	
Imp ₇	-1.97	0.198	-0.131	0.136	-	0.139	0.89	8.1%	-187	0.011	
P	-1.33	0.183	-0.111	0.097	-0.172	-	0.90	7.9%	-188	0.005	
P ₂₂₄	-1.76	0.190	-0.116	0.125	-0.170	-	0.91	7.6%	-192	<0.001	

(i) For day1 Eqs. (18) and (19)

Impervious-											
ness								Adjusted	Standard	p-values for	
Variable	Incpt	a	p	yr	dd	srf	imp _x	R ² (a)	Error (b)	AIC _c (c)	Imp _x
	(-)	(mi ²)	(in.)	(yrs)	(mi/mi ²)	(-)	(-)				
Imp _{av}	-12.9	0.676	3.71	1.85	-	-	13.8	0.75	92%	709	0.002
Imp ₅	-13.3	0.706	3.75	1.92	-	-	1.79	0.76	89%	707	< 0.001
Imp ₇	-13.6	0.727	3.78	2.00	-	-	2.08	0.77	85%	702	< 0.001
Imp _{av}	-9.55	0.905	2.25	1.84	-1.56	5.54	12.7	0.81	66%	686	0.001
Imp ₅	-10.1	0.924	2.37	1.90	-1.57	5.31	1.63	0.82	65%	685	< 0.001
Imp ₇	-10.4	0.945	2.40	1.93	-1.59	5.32	1.92	0.83	67%	687	< 0.001

Table 4. Continued

(j) For day2 Eqs. (20) and (21)

Impervious-ness or Precipitation Variable	Incpt (-)	$\beta_{Q_{10}}$ (cfs)	β_{day1} (days, cfs)	β_{yr} (yrs)	β_{Px} (in.)	β_{Impx} (-)	Adjusted R^2 ^(d)	Standard Error ^(b)	AIC _c ^(c)	p-values for Imp _x or P _x
Imp _{av}	-1.60	0.166	-0.138	0.129	-	0.720	0.85	9.1%	-188	0.060
Imp ₅	-1.63	0.169	-0.139	0.134	-	0.089	0.85	9.1%	-188	0.058
Imp ₇	-1.65	0.170	-0.140	0.140	-	0.106	0.85	9.1%	-188	0.044
P	-1.22	0.157	-0.123	0.102	-0.098	-	0.84	9.2%	-187	0.096
P ₂₂₄	-1.40	0.154	-0.111	0.107	-0.167	-	0.87	8.3%	-195	0.013

^(a) Adjusted R^2 reported from geometric space^(b) Standard Error of estimate expressed as percentage of sample mean in arithmetic space^(c) Corrected AIC reported from arithmetic space^(d) Adjusted R^2 reported from arithmetic space (for linear models)

Equation (7) is presented with corresponding parameters, units, and performance measures in Table 4(b):

$$Q_i = e^{(Incpt)*} A^a * DD^{dd} * P_{224}^{p224} * Imp_{max}^{impmax} \quad \text{Eq. (7)}$$

where:

A = total contributing drainage area (mi²);DD = drainage density computed by total stream length divided by drainage area (mi/mi²);P₂₂₄ = 2-yr 24-hr precipitation volume: NRCS (in.);Imp_{max} expressed as **percentage** of total drainage area (mi²/mi²) * 100%; andImp_{max} ≥ 1% or else term is dropped.

Equation (8) is presented with corresponding parameters, units, and performance measures in Table 4(c):

$$Q_i = e^{(Incpt)*} Stm^{stm} * P_{224}^{p224} * e^{(impmax*Impmax)} \quad \text{Eq. (8)}$$

where:

Imp_{max} expressed as **fraction** of total drainage area (mi²/mi²).

Equation (9) is presented with corresponding parameters, units, and performance measures in Table 4(d):

$$Q_i = e^{(Incpt)*} A^a * P_{224}^{p224} * Elv_{bsn}^{elv} * e^{(impmax*Impmax)} \quad \text{Eq. (9)}$$

where:

Elv_{bsn} = average elevation between the 10 and 85% points along the main channel

from outlet to divide (feet above mean sea level); and

Imp_{max} expressed as **fraction** of total drainage area (**mi²/mi²**).

Equation (10) is presented with corresponding parameters, units, and performance measures in Table 4(e):

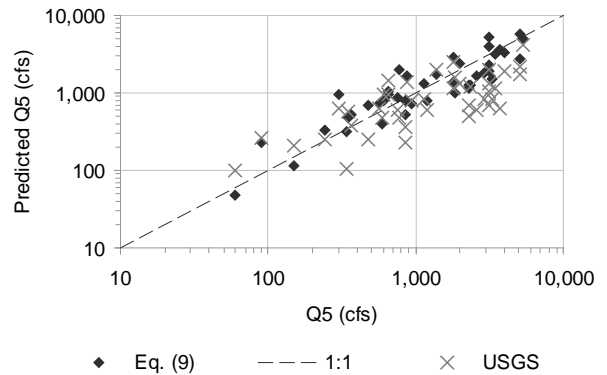
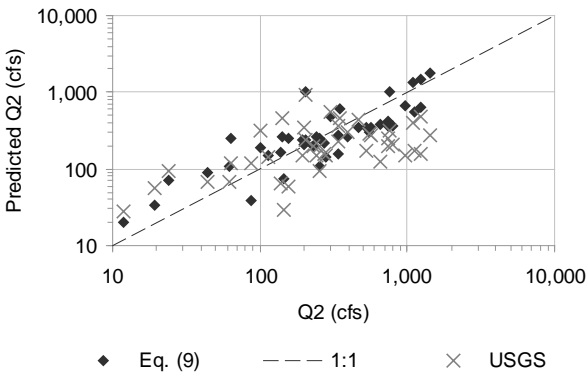
$$Q_i = e^{(Incpt) * A^a * P^p * e^{(impmax * Impmax)}} \quad \text{Eq. (10)}$$

where:

P = average annual precipitation, USGS: 1900 - 1960 (in.); and

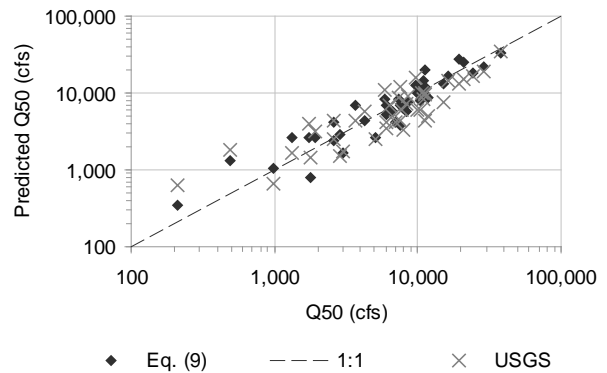
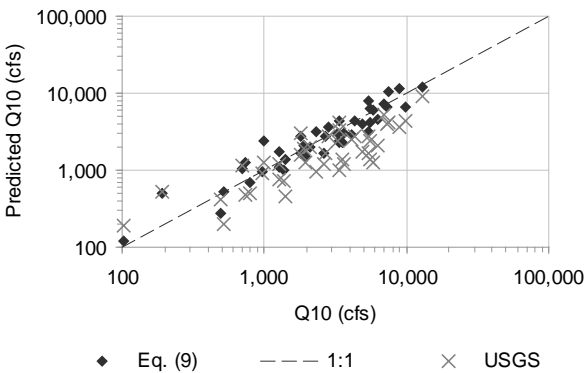
Imp_{max} impervious area as **fraction** of total drainage area (**mi²/mi²**).

Model performance generally increases up to Q₁₀, with relatively consistent precision at higher return intervals. Performance of Eq. (9) relative to the USGS rural (1977) and urban (1983) equations is depicted in Figures 12 and 13, respectively. The disparity between our models and the USGS models decreases with increasing return period (Table 5).



(a) at Q2

(b) at Q5



(c) at Q10

(d) at Q50

Figure 12. Comparison of performance between Eq. (9) and USGS rural (1977).

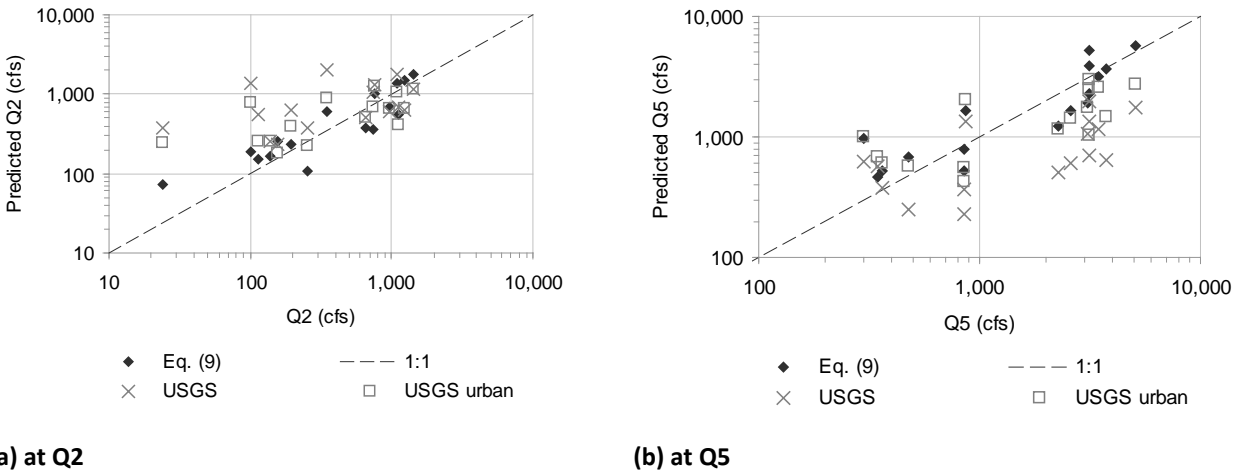


Figure 13. Comparison of performance between Eq. (9) and USGS urban (1983) in most urbanized watersheds.

Table 4. Comparison of Q_i model performance with USGS rural (1977) and urban (1983) equations using Standard Error values from arithmetic space.

Return Period (yrs)	Standard Error of Estimate as % of Sample Mean (arithmetic space)					USGS1977 Rural	USGS 1983 Urban
	Eq. (6)	Eq. (7)	Eq. (8)	Eq. (9)	Eq. (10)		
1.5	68%	94%	83%	67%	85%	-	-
2	62%	82%	74%	63%	76%	104%	91%
5	49%	59%	56%	47%	59%	80%	80%
10	39%	41%	40%	34%	45%	67%	78%
25	39%	32%	32%	32%	37%	51%	70%
50	42%	31%	31%	34%	37%	43%	64%
100	45%	32%	33%	37%	38%	40%	60%

Given the longer records and a focus on smaller watersheds, our models generally outperform the USGS equations (Table 5). It should be noted that the SE for the USGS urban equation is substantially influenced (perhaps unduly) by the large number of predictor variables (seven) relative to the sample size. However, direct comparisons of unadjusted metrics such as R^2 or Sum of Squared Errors (SSE) demonstrated better performance by our equations in every case relative to the USGS urban equations. The single case where our equations were outperformed by the USGS rural equations was Eq. (6) at the 100-yr flow, which is included because it was one of the best performing equations at $Q_{1.5}$ through Q_{10} .

Duration Density Functions

Power functions (Eqs. (4) and (5)) are used to predict durations of bin flows as scaled by Q_{max} using Eq. (1). Two forms of the power function cover different ranges of bins (i.e., bins 16-25 with d_1 and d_2 or

bins 12-25 using day1 and day2). Models for each are presented with Q_{\max} followed by d1 and d2, followed in turn by day1 and day2.

Models of Q_{\max} (cfs) that were advanced from cross validation performed comparatively well during final calibration in both geometric and arithmetic space. The only notable change was that DD and Yr became less significant, with p-values greater than 0.05 in some cases. Final models are presented with corresponding parameters, units, and performance measures in Table 4(f):

$$Q_{\max} = e^{\text{Incpt}} * A^a * P_x^{\text{px}} * Yr^{\text{yr}} \quad \text{Eq. (11)}$$

$$Q_{\max} = e^{\text{Incpt}} * A^a * P_x^{\text{px}} * Yr^{\text{yr}} * DD^{\text{dd}} \quad \text{Eq. (12)}$$

$$Q_{\max} = e^{\text{Incpt}} * \text{Stm}^{\text{stm}} * P_x^{\text{px}} * Yr^{\text{yr}} \quad \text{Eq. (13)}$$

where:

- Q_{\max} = maximum mean 24-hr flow (cfs);
- Yr = length of mean-daily flow record (yrs);
- P_x = P or P_{224} (as specified in Table 4(f)), where:
 - P = mean annual precipitation 1900 - 1960 (USGS) (in.); and
 - P_{224} = 2-yr 24-hr precipitation volume (NRCS) (in.).

A substantial outlier was identified during the cross-validation phase of d1, and confirmed during final calibration *across all model forms*. Consistently outside of the 95% confidence interval for model predictions, studentized residuals ranged from -2.5 to -4, while other points generally fell within -2 to 2. The 'best' case for its inclusion was model d1 = $f(A, DD, \text{Srf}, \text{Yrs}, \text{Imp}_{\text{av}})$, with a Cook's D of 0.39 and an RStudent residual of -3.0, corresponding to a two-sided p-value of 0.005. Because the coefficient of the DDF was suspected to be atypically low *a priori*, a one-sided p-value could be justified (i.e., 0.0026). However, Cook's D and the Rstudent residual were usually far worse, ranging up to 1.0 and -5.1, respectively, in model d1 = $f(A, P, \text{Yrs}, \text{Imp}_7)$, corresponding to a two-sided p-value of 0.00001, which clearly justified its removal during final calibration.

The base model d1 = $f(A, P, \text{Yr}, \text{Imp}_x)$, performed relatively well in geometric space; however, arithmetic space performance was significantly improved by adding Srf and DD. Given that the expanded model offered slightly more homoscedastic residuals and all variables were significant ($p < 0.05$) during both cross validation and final calibration, we include it as an alternative to the four-term model. Equations are presented with corresponding parameters, units, and performance measures in Table 4(g). The relatively-large standard errors in arithmetic space are somewhat misleading because the appropriate scales are geometric, varying over three orders of magnitude (300 - 360,000).

$$d_1 = e^{(\text{incpt})} * A^a * P^p * Yr^{\text{yr}} * e^{(\text{imp}_x * \text{Imp}_x)} \quad \text{Eq. (14)}$$

$$d_1 = e^{(\text{incpt})} * A^a * P^p * Yr^{\text{yr}} * DD^{\text{dd}} * e^{(\text{srf} * \text{Srf})} * e^{(\text{imp}_x * \text{Imp}_x)} \quad \text{Eq. (15)}$$

where:

- Srf = average surface slope of watershed (m/m); and
- Imp_x** = Imp_{av}, Imp₅, or Imp₇ (as specified in Table 4(g)), where:
- Imp_{av}** = average impervious extent over record as a fraction of total drainage area (**mi²/mi²**);
- Imp₅** = fraction of record greater than 5% TIA (**yr/yr**); and
- Imp₇** = fraction of record greater than 7.5% TIA (**yr/yr**).

As during the cross-validation phase, the majority of the variance in d2 was explained by d1, Q₁₀, and Yr (in that order). In the fourth position, both impervious and precipitation terms accounted for similar proportions of the variance, while no additional variables were significant. Performance measures such as R² and SE slightly favored the models that included precipitation in the place of imperviousness. In contrast, however, residuals relative to predicted values were more equitably distributed by including imperviousness.

With similar performance across several measures, alternatives of the linear base model ($d_2 = f(Q_{10}, d_1, Yr)$) developed in arithmetic space are presented, with corresponding parameter values and performance measures in Table 4(h).

$$d_2 = \text{Incpt} + \beta_{Q_{10}} * \ln(Q_{10}) + \beta_{d_1} * \ln(d_1) + \beta_{Yr} * \ln(Yr) + \beta_{\text{imp}_x} * \text{Imp}_x \quad \text{Eq. (16)}$$

$$d_2 = \text{Incpt} + \beta_{Q_{10}} * \ln(Q_{10}) + \beta_{d_1} * \ln(d_1) + \beta_{Yr} * \ln(Yr) + \beta_{P_x} * \ln(P_x) \quad \text{Eq. (17)}$$

where:

- Q₁₀ = 10-yr instantaneous peak flow (cfs); and
- d1 = coefficient of DDF calibrated in 'days' and 'cfs'.

As with d1, models of day1 explained the most variance and had greatest homoscedasticity using the exponential forms of imperviousness as opposed to power forms. Standard diagnostics showed similar performance with each impervious measure (i.e., Imp_{av}, Imp₇, and Imp₅), justifying the inclusion of all three forms. The six-term model performed the best in both cross validation and final calibration, with all terms significant ($p < 0.05$) and the greatest homoscedasticity. Furthermore, the case could be made that this form of model offers a more complete representation of the effect of urbanization. That is, imperviousness is still predicted to have an exponential effect on days of occurrence even after accounting for the wide range of other theoretically-important, relatively-significant variables. As such, we include them as alternatives to the more heuristic four-term models. Day1 equations are presented with corresponding parameters, units, and performance measures in Table 4(i). The smaller (arithmetic space) standard errors in comparison to d1 are more attributable to the smaller day1 range (100 to 60,000) than substantial improvements in performance:

$$\text{day}_1 = e^{(\text{incpt}) * A^a * P^p * Yr^{yr} * e^{(\text{imp}_x * \text{Imp}_x)}} \quad \text{Eq. (18)}$$

$$\text{day}_1 = e^{(\text{incpt}) * A^a * P^p * Yr^{yr} * DD^{dd} * e^{(\text{srf} * \text{Srf})} * e^{(\text{imp}_x * \text{Imp}_x)}} \quad \text{Eq. (19)}$$

Day2 had three consistently significant predictor variables: Q_{10} , day1, and Yr. The placeholder for the fourth variable was tested with all remaining independent variables; however, similar to the d2 models, the best performance was achieved with measures of imperviousness or precipitation. Residual patterns relative to Q_{10} were less pronounced than during cross validation, with impervious models slightly more patterned than those that included precipitation measures. Equation formats are presented with corresponding parameters, units, and performance measures in Table 4(j):

$$\text{day}_2 = \text{Incpt} + \beta_{Q_{10}} * \ln(Q_{10}) + \beta_{\text{day1}} * \ln(\text{day1}) + \beta_{yr} * \ln(Yr) + \beta_{\text{imp}_x} * \text{Imp}_x \quad \text{Eq. (20)}$$

$$\text{day}_2 = \text{Incpt} + \beta_{Q_{10}} * \ln(Q_{10}) + \beta_{\text{day1}} * \ln(\text{day1}) + \beta_{yr} * \ln(Yr) + \beta_{P_x} * \ln(P_x) \quad \text{Eq. (21)}$$

where:

Q_{10} = 10-yr instantaneous peak flow (cfs); and

day1 = coefficient of DDF calibrated in 'days' and 'cfs'.

Implications and Discussion

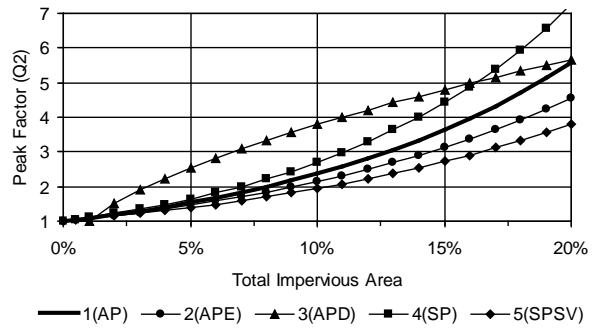
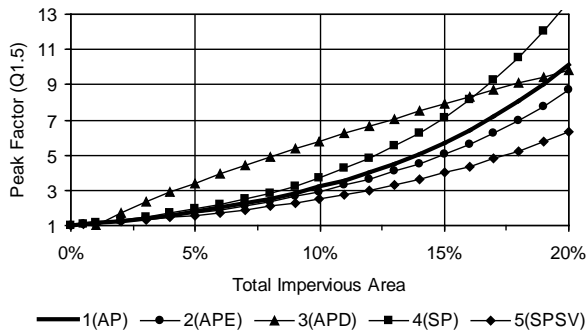
The models predict higher peak flows (especially for $\leq Q_5$), and longer durations across all sediment-transporting flows in urban watersheds. As an example, we applied them to a hypothetical watershed with average conditions, controlling for everything but imperviousness. Beyond model application, case studies are presented of two gauges whose records spanned periods of relatively undeveloped and developed periods, offering support to the broader statistical models. Finally, recall that the models were developed using gauges ranging in drainage area from 0.5 to 105 mi² with 0 to 26% TIA (Table 1); therefore, the equations should not be applied to watersheds outside of those bounds. Regarding DDFs, models were calibrated with gauges that had a positively-skewed range of ~20 to 95 yrs with a mean of ~45 and standard deviation of ~20. In application, we recommend simulations within one standard deviation of the mean (i.e., ~25 to 65 yrs, convenient for the typical engineering time frame of ~50 yrs).

Effects of Urbanization Predicted by Models

Large increases were found in instantaneous-peak flows of more frequent return periods relative to a rural setting of $\leq \sim 1\%$ imperviousness. The effects of urbanization decreased with larger, less frequent storms. For example, median peak factors for a watershed with 20% imperviousness were $\sim 10x$, $\sim 6x$, and $\sim 2x$ for the 1.5-, 2-, and 5-yr flows, respectively (Figure 14). Such attenuating influence of urbanization with return period is generally consistent with both theory and previous studies (Bledsoe and Watson, 2001; Hollis, 1975; Sauer *et al.*, 1983), including studies specific to California (Rantz, 1971) and southern California (Durbin, 1974). Fundamental hydrology suggests that during very large, infrequent events (e.g., Q_{100}) soils have become saturated and behave similar to impervious surfaces.

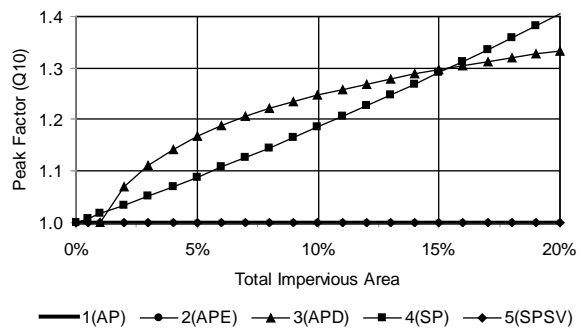
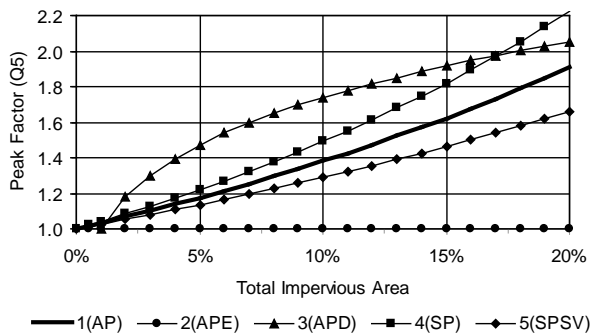
The peak factors presented here are generally larger than those from previous studies. For example, Hammer (1972) and Hollis (1975) suggested that the 1.5- to 2-yr flows could double or triple at 10 to 20% imperviousness, and Bledsoe and Watson (2001) found peak factors ranging 1.5 to 4 dependent on regional setting. At those same impervious ranges and flow intervals, median-peak factors from the models ranged 3 to 10, with the maximum projected increase of 7x at Q_2 and 14x at $Q_{1.5}$ with 20% imperviousness. Though such increases may seem extreme, they are not the largest that have been reported (e.g., Urbonas and Roesner (1993)). The flashiness of the setting combined with limited flow-control practices suggest that peak factors of southern California could be larger than in other regions, although the relatively small basin sizes from this study may also play a factor in the higher peak factors.

Models of 1-yr flows performed poorly overall and are not reported, but the influence of urbanization was nevertheless unequivocal. Despite fifteen of the forty-three gauges having a Q_1 of 0 cfs (range 0 to 236, median 1.8, and mean of 14 cfs) the four most urban gauges (Imp_{av} 9 to 14%) accounted for the four largest 1-yr flows (i.e., 236, 102, 49, and 26 cfs) over records of 23 to 43 yrs.



(a) at Q_{1.5}

(b) at Q₂



(c) at Q₅

(d) at Q₁₀

Model Key: 1 = $f(A, P, Imp_{max})$

2 = $f(A, P_{224}, Elv, Imp_{max})$

3 = $f(A, P_{224}, DD, Imp_{max})$

4 = $f(Stm, P_{224}, Imp_{max})$

5 = $f(Stm, IP, Shp, Vly, Imp_{max})$

Figure 14. Peak factors for instantaneous peak flows as a function of TIA for all five calibrated peak flow models: (a) at Q_{1.5}, (b) at Q₂, (c) at Q₅, (d) at Q₁₀.

Finally, regarding peak-flow models, the fact that Imp_{max} accounted for more variance than other impervious measures such as Imp_{av} , Imp_5 , or Imp_7 , shows the ease at which the most developed portion of a gauge record can overwhelm the undeveloped peak flows, especially for the more frequent return intervals. It may suggest the potential for a statistically-significant influence at higher return intervals (e.g., Q_{10}) in the future as gauges have more time to record large precipitation events at those impervious levels.

Regarding the DDF curves, gauge data to date did not show urbanization as statistically significant in explaining their scale (Q_{max}), but it had an exponential effect on the magnitude (d1 and day1, i.e., number of days), with a linear effect on d2 and day2 (shape). The combined effect tends to magnify durations of the moderate flows slightly more than durations of the largest flows. Figure 15 presents a 25-yr simulation of an average watershed across rural and urban scenarios using both models (i.e., d1/d2, bins 16-25 and day1/day2, bins 12-25) demonstrating relatively good agreement. Differing only by levels of imperviousness (i.e., Imp_{av} 12% versus 0.5%), the urban setting showed a 3-fold increase in the number of expected days at 50 cfs, with a 2- to 2.4-fold increase at 850 cfs (Table 7).

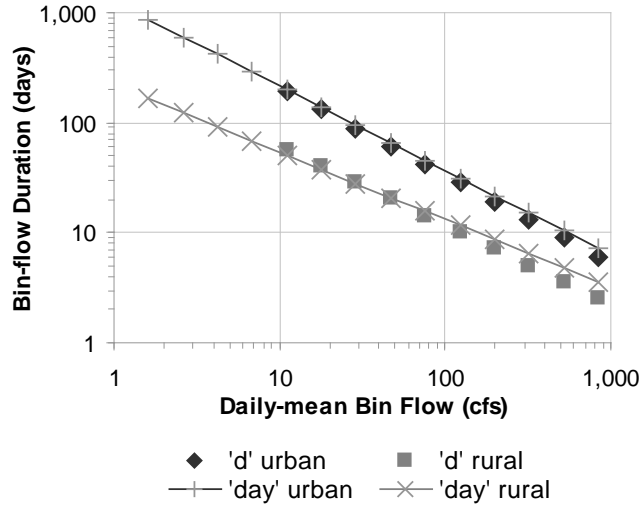


Figure 14 – DDFs of 25-yr simulations of equivalent watersheds in rural and urban settings

Table 5 – Summary of 25-yr DDF simulation for ‘dry’, rural, and urban scenarios in an average^(a) watershed

Variable		Rural	Urban	Ratio (Urban/Rural)
key values for DDF model input	Imp _{av}	0.5%	12%	
	Q _{max} (cfs)	1,040	1,040	1
	Q ₁₀ (cfs)	2,470	2,730	1.1
d1/d2 model	d1	326	1,330	4.1
	d2	-0.72	-0.80	1.1
	days @ ~10 cfs (bin 16)	57	194	3.4
	days @ ~50 cfs (bin 19)	20	61	3.0
	days @ ~125 cfs (bin 21)	10	28	2.8
	days @ ~320 cfs (bin 23)	5.0	13	2.6
	days @ ~850 cfs (bin 25)	2.5	6.1	2.4
day1/day2 model	day1	221	1,260	5.7
	day2	-0.61	-0.77	1.3
	days @ ~10 cfs (bin 16)	51	199	3.9
	days @ ~50 cfs (bin 19)	21	66	3.1
	days @ ~125 cfs (bin 21)	12	31	2.7
	days @ ~320 cfs (bin 23)	6.4	15	2.3
	days @ ~850 cfs (bin 25)	3.6	7.2	2.0

^(a) ‘average’ watershed (A ~30 mi², P ~14 in., DD ~1.9 mi/mi², Srf ~18%)

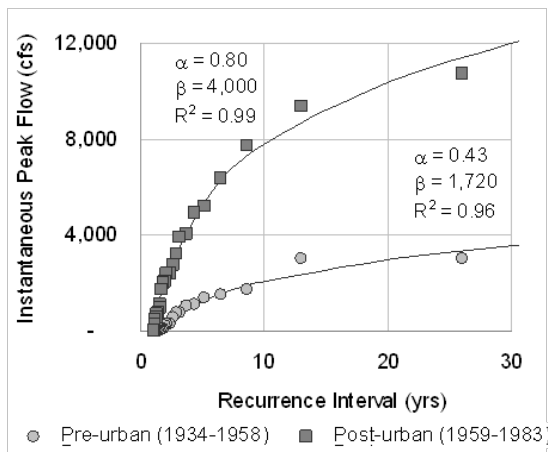
Alternative urban scenarios predict similarly disproportionate increases in durations. For example, 5% imperviousness would increase durations of bin 16 by ~1.5 and bin 25 by ~1.3, while 15% imperviousness would result in ~4.1 and ~2.4-fold increases, respectively. These empirical findings of decreasing influence of urbanization on flow duration with increasing flow magnitude are consistent

with the findings regarding peak flows: urbanization tends to show higher influence on more frequent events, with decreasing influence over the largest, rarest storms.

In conclusion, the fact that Imp_{av} , Imp_7 , and Imp_5 outperformed Imp_{max} in DDF models suggests that it may take longer for urbanization to show an effect on the cumulative durations of all flows than to appreciably affect instantaneous peaks at small return intervals. Relatively low measures of imperviousness (i.e., $< 5\%$) did not show as strong of a statistically-significant influence on durations as on peak flows; however, above 5% and especially above 7.5% there was an unmistakable influence. From this, we are not suggesting that above 5 or 7.5% imperviousness all watersheds behave identically, but rather that it is more difficult for the models to discern differences in durations below those thresholds with current data.

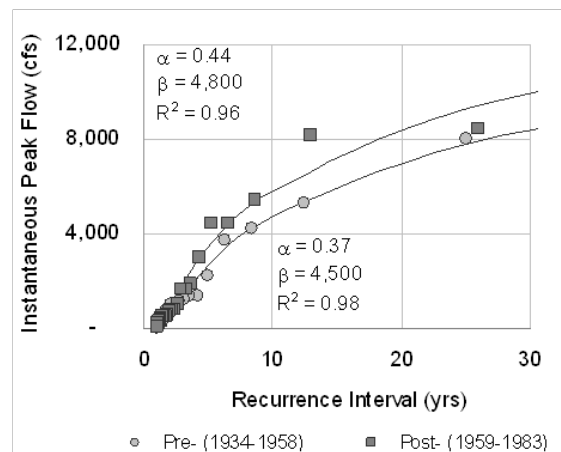
At-a-station effects of urbanization

Two gauges (Arroyo Simi in Ventura County and San Diego Creek in Orange County) spanned equal periods of relatively undeveloped and developing/developed states such that they could be divided into ‘pre-urban’ and ‘post-urban’ samples. The paired data showed a marked influence across all peaks and durations of record. For example, Arroyo Simi, depicted in Figure 16(a), had more than a 10-fold difference in the 2-yr flow (2,040 cfs versus 174 cfs), while the 25-yr flow was over three times as large at 10,700 cfs relative to 3,000 cfs. Figure 15(b) summarizes the record at the rural gauge of Hopper Creek spanning the same time frame. By comparison, peak flows differed by an average of only 20% across the two periods in the rural setting, and are likely attributable to the variability in the inter-period precipitation.



1934-1958: $Imp_{av} = 2.6\%$, $Imp_{max} = 4.7\%$
 1959-1983: $Imp_{av} = 7.3\%$, $Imp_{max} = 8.6\%$

(a) recorded at Arroyo Simi during the pre-urban and post-urban periods

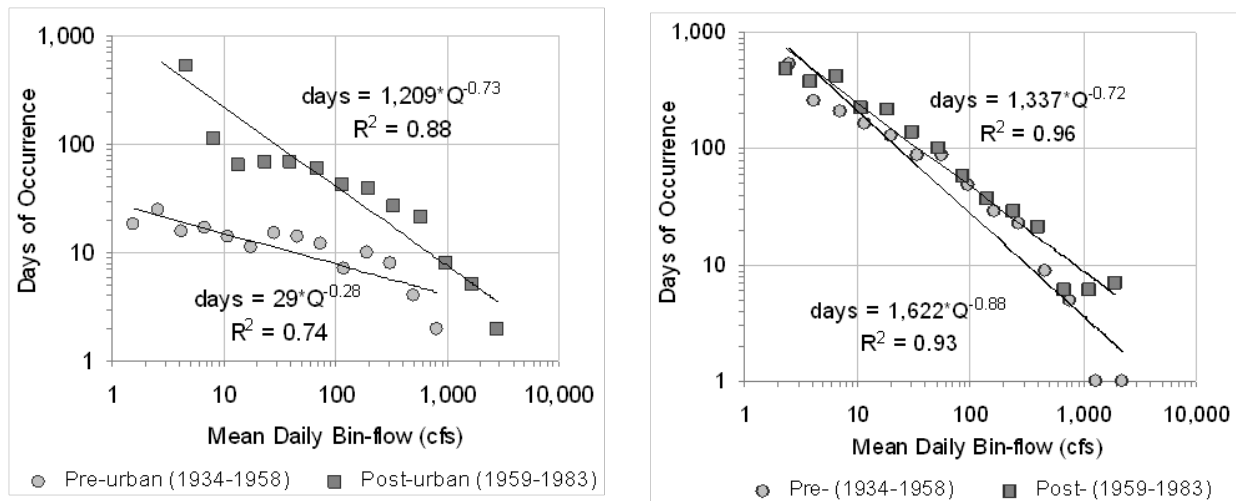


1934-1958: Imp_{av} and $Imp_{max} = 0.0\%$
 1959-1983: Imp_{av} and $Imp_{max} = 0.0\%$

(b) recorded at Hopper Creek covering the same periods with no urbanization

Figure 16 – Instantaneous-peak flow relative to recurrence interval, with fitted gamma distributions

The long-term durations of daily-mean flows were also clearly affected by the change in land use at Arroyo Simi and San Diego. Figure 17(a) presents the respective DDFs of Arroyo Simi, recording both higher flows and longer durations for the urban regime. The maximum daily discharges over the 24.5-yr periods were 1,000 and 3,610 cfs, respectively, with the undeveloped regime incurring only 4 days at 500 cfs and 2 days at 800 cfs, while the post-developed regime had 21 days at 600 cfs and 8 days at 1,000 cfs. Additionally, 5 days at 1,700 cfs and 2 days at 2,900 cfs were recorded during the post-urban period, with no days of comparable flows in the pre-urban period. Presuming sediment is entrained by these higher flows, the post-developed regime had on average four to five times as many days of sediment-transporting flows as the pre-developed case, with an additional 7 days of flows that far exceeded the maximum flow in the undeveloped setting.



(a) at Arroyo Simi during the pre-urban and post-urban periods

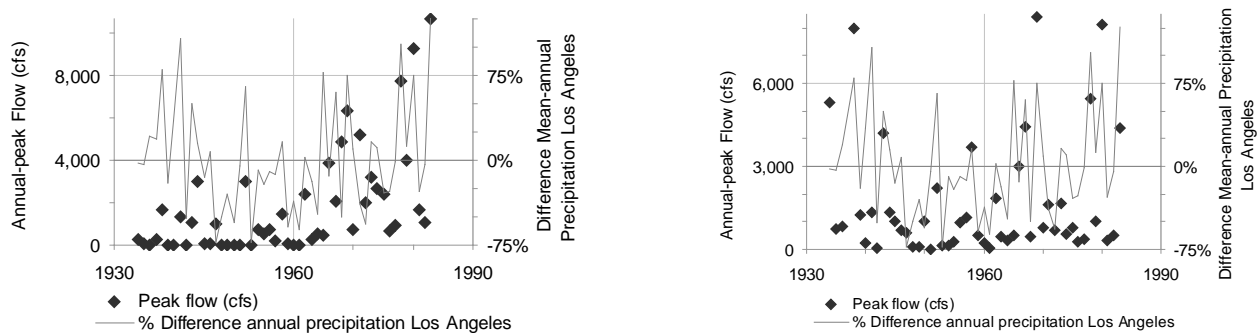
(b) at Hopper Creek covering the same periods with no urbanization

Figure 15 – Cumulative-duration histogram centroids, with fitted DDFs

In contrast, bin flows and durations during the same two periods at the undeveloped gauge were relatively similar. Figure 17(b) presents the nearly overlaid DDFs of Hopper Creek, with all but the two largest bins differing by an average of only 50%. The latter period experienced 6 days at 1,100 cfs and 7 days at 1,900 cfs, while the earlier period only had 1 day at each of the corresponding bins of 1,300 and 2,200 cfs. Even so, the maximum-daily flow was actually largest in the ‘pre-’ period (2,770 cfs versus 2,400 cfs).

In summary, the rural gauge had a small vertical shift in the DDF between the two periods with slightly more days of similar flows. However, the urban gauge showed dramatic shifts in the DDF both vertically and laterally. At both San Diego and Arroyo Simi, Q_{\max} increased by a factor of 3 to 4, while durations of corresponding bin flows increased by factors of 3 to 6 from the undeveloped to urban portions of the records.

We considered potential differences in climate as a competing hypothesis as opposed to urbanization as the primary cause of increased flows and durations between the two periods. As seen in Figure 18(a), the pre-urban period of Arroyo Simi (1934 - 1958) begins with relatively wet years and trends downward, while the post-urban period (1959 - 1983) begins in a relative drought and trends upward. Although the higher peak flows in the respective periods generally correspond with exceptionally wetter years, precipitation alone clearly cannot explain the somewhat flat trend in peak flows during the pre-urban period and the largely upward trend during the post-urban period. In contrast, the relative similarity among the highest peaks between the same two periods at the rural gauge of Hopper Creek (Figure 17(b)) and better correlation with the higher precipitation years adds support for causation between urbanization and the latter-period extreme flows recorded at Arroyo Simi.



(a) recorded at Arroyo Simi
(urban during second half of record)

(b) recorded at Hopper Creek
(rural)

Figure 16 – Annual peak flows overlaid with relative difference in mean-annual precipitation at the Los Angeles weather station

By tracking urbanization through time via impervious cover, the positive trend in peak flows at Arroyo Simi is much better explained (Figure 19). Indeed, multivariate at-a-station regression can explain up to 60% of the variance in annual-peak flows at Arroyo Simi by including imperviousness and annual precipitation as recorded at Los Angeles, with imperviousness highly significant ($p < 0.0001$) and accounting for 30 to 40% of the total variance.

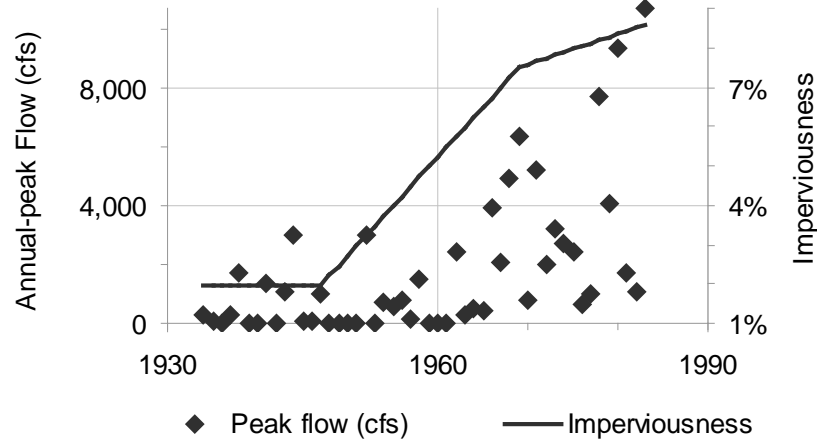


Figure 17 – Annual peak flows recorded at Arroyo Simi overlaid with interpolated percentage of impervious cover in the watershed as tracked via historic USGS quadrangle maps

As indicated in Table 8, the urban records did correspond to periods of slightly higher precipitation in terms of the annual precipitation at the Los Angeles weather station and number of exceptionally wet and dry years. However, these climatic differences alone cannot explain the dramatic differences in flows and durations. The post-urban period of Arroyo Simi has nine flows larger than the largest instantaneous-peak flow from the pre-urban period. In the case of San Diego, there were five flows higher than the maximum from the pre-urban regime. By comparison, the rural gauge at Hopper Creek had only two flows during the latter period that were higher than the highest peak from the first half of the record and they differed by only 5% (i.e., 8,400 and 8,120 cfs versus 8,000 cfs). Also recall that the rural gauge recorded a higher Q_{max} and only slightly less (50%) days of equivalent flows during the earlier period, compared with 3- to 5-fold duration increases at the urban gauges with substantially larger values of Q_{max} .

Table 6 – Comparison of flows, durations, climate, and imperviousness over the pre-urban and post-urban periods of Arroyo Simi (Ventura County) and San Diego Creek (Orange County)

Variable/ Value	Arroyo Simi (Ventura County)			San Diego Creek (Orange County)			
	Pre-urban	Post-urban	Post/ Pre	Pre-urban	Post-urban	Post/ Pre	
	1934 - 1958	1959 - 1983		1950 - 1967	1968 - 1985		
Return Interval	Flow Pre	Flow Post	Ratio	Flow Pre	Flow Post	Ratio	
(yrs)	(cfs)	(cfs)		(cfs)	(cfs)		
peak flows	1	-	14	∞	-	448	∞
	1.5	19	891	> 40	726	1,233	1.7
	2	174	2,040	12	907	1,937	2.1
	5	1,278	5,138	4.0	1,932	6,363	3.3
	10	2,059	7,790	3.8	2,910	8,192	2.8
	25	3,305	11,237	3.4	4,025	11,625	2.9
	50	4,301	13,877	3.2	4,866	14,237	2.9
	100	5,326	16,536	3.1	5,704	16,859	3.0
durations	~ Mean Daily Flow	Days Pre	Days Post	Ratio	Days Pre	Days Post	Ratio
	(cfs)	(#)	(#)		(#)	(#)	
	100	7	42	6.0	9	37	4.1
	200	10	39	3.9	6	32	5.3
	400	8	27	3.4	8	26	3.3
	600	4	21	5.2	3	9	3.0
	800	2	8	4.0	-	10	∞
	1,700	-	5	∞	-	6	∞
2,900	-	2	∞	-	-	∞	
extreme flows and Los Angeles precipitation^(a)	Variable	Pre	Post	Ratio	Pre	Post	Ratio
	(unit)	(varied units)	(varied units)		(varied units)	(varied units)	
	mean annual precip. (in)	15.0	15.7	1.04	13.4	16.0	1.2
	'wet' years (#)	3	6	2	3	4	1.3
	'high' peaks (#)	2	10	5	1	6	6.0
	'dry' years (#)	4	3	0.75	4	1	0.25
'low' peaks (#)	18	8	0.44	11	5	0.45	
impervious-ness	Spatial Extent During Period	TIA Pre	TIA Post	Ratio	TIA Pre	TIA Post	Ratio
		(%)	(%)		(%)	(%)	
	maximum	4.7	8.6	1.8	3.2	14.9	4.5
mean	2.6	7.2	2.8	3.2	9.7	2.9	

^(a) 'wet' and 'high' correspond to years/events 50% greater than the respective means, while 'dry' and 'low' indicate years/events 50% lower than the mean

The differences in flows and durations between undeveloped and developed periods at the same gauges and the relative similarity during the same periods at the rural gauge add to the weight of evidence that such changes are largely attributable to urbanization. In fact, these differences observed at individual gauges were larger than what is predicted in the models, particularly in terms of Q_{\max} . The effects of urbanization captured in the models may have been dampened by the widespread variability across all sites, most of which were still relatively undeveloped. As more years of data are gathered at urban gauges, the models could be further refined to account for urbanization with a more equitable sampling of urban data.

Summary and Conclusions

The overarching objective of this paper was to understand the effects of urbanization on the magnitude and duration elements of flow regimes (i.e., 'hydromodification') in southern California. In doing so, updated alternatives to the USGS regional equations were developed for peak flows, which outperformed both rural (Waananen and Crippen, 1977) and urban (Sauer *et al.*, 1983) models in twenty-nine out of thirty cases in terms of Standard Error, Adj. R^2 , etc. The difference was particularly substantial for more frequent return periods (e.g., Adj. R^2 in arithmetic space ~ 0.7 to 0.8 versus < 0.4 at Q_{10}).

Additionally, our models documented changes in the significance of individual variables with return period, reflecting shifts in physical processes. For example, at more frequent events, the efficiency with which a drainage network concentrated and conveyed runoff became increasingly significant in predicting peak flow, while the predominant variables at less frequent events were measures of watershed size and precipitation volume. This may point to different model forms for different return intervals, for example using Eq. (6) to estimate flows less than or equal to Q_5 , and Eq. (8) or (10) for Q_{10} and higher.

Beyond peak flows, we developed a method for estimating long-term cumulative durations at ungauged sites. DDFs expand on previous approaches to histogram-style duration curves in that their magnitude, shape, and scale are based on watershed physical properties rather than scaling based on a nearby gauge and a single flow. Most importantly regarding hydromodification, both the peak flow and DDF models account for urbanization using measures of total impervious area, which were statistically significant ($p < 0.05$), particularly for peak flows $\leq Q_2$ and the magnitude (coefficient) component of DDFs, resulting in longer durations across all flows greater than some nominal value (e.g., 1 to 10 cfs).

Multivariate regression controlling for other potentially-significant hydro-climatic variables (e.g., drainage area, mean annual rainfall, surface slope, etc.) correlated urbanization to higher peaks and longer durations of all geomorphically-significant flows. These effects were also documented at individual gauges whose records spanned both pre-urban and post-urban periods. Moreover, these effects were not linear. Although several metrics, units, and equation forms were tested for modeling the effects of urbanization, the form that was most powerful was typically the exponential of total imperviousness as a fraction of the drainage area. That is, flow magnitudes and durations associated with identical watersheds differing only by measures of imperviousness (e.g., $\sim 1\%$ and $\sim 10\%$) would be

disproportionately larger. In terms of peaks, differences would be most substantial at the more frequent events (e.g., $\sim 3.2 \times Q_{1.5}$, $\sim 2.4 \times Q_2$, and $\sim 1.4 \times Q_5$). Regarding durations of daily-mean flows, ~ 2 to 4 times as many days of *all* sediment-transporting flows would be predicted, with the largest increases occurring at more frequent events and smaller but significant increases at the most infrequent events.

Such changes in the hydrologic regime can have far-reaching effects on receiving channels in terms of cumulative erosive energy and channel stability. Particularly for channels considered highly susceptible to hydromodification (e.g., live-bed unconfined systems), significant changes in channel form such as incision, widening, or planform shifts are anticipated if land-cover conversions from pervious to impervious go unmitigated. The relatively-dramatic responses in channel form that have been observed throughout the region are better explained in the context of such equally compelling changes in flow rates and durations of sediment-transporting events. The physically-based, empirically-calibrated hydrologic models presented here may become important tools in developing a process-based understanding of hydromodification effects on fluvial systems in southern California.

Future Work

The logical next step is to apply these hydrologic models to sites where geomorphic data have been collected to evaluate whether changes in flows correspond to sediment discontinuities that in turn correlate to channel degradation. For example, can risk-based models of channel stability be developed using these hydrologic models as a starting point?

Future work could also focus on the refinement of the DDF models developed in this paper. For example, we were limited to daily-mean flow data for these analyses, but one could follow up with the USGS in a subsequent study to see if any of the gauges have 15-min or hourly data over their entire record (i.e., twenty of the fifty-two gauges were 'real-time' sites offering 15-min data for the last 60 days but only daily data over extended records). If one could acquire the finer resolution data for enough sites, they could repeat the histogram procedure in the hope of developing a scaling factor for the DDFs in this paper.

References

- Alley, W.A., Veenhuis, J.E., 1983. Effective impervious area in urban runoff modeling. *Am. Soc. Civil Eng., J. Hydrol. Eng.* 109(2), 313-319.
- Biedenharn, D.S., Copeland, R.R., Thorne, C.R., Soar, P.J., Hey, R.D., Watson, C.C., 2000. Effective Discharge Calculation: A Practical Guide. ERDC/CHLI TR-00-15, U.S. Army Corps of Engineers, Engineer Research and Development Center, Coastal and Hydraulics Laboratory, Vicksburg, Miss.
- Biedenharn, D.S., Thorne, C.R., Soar, P.J., Hey, R.D., Watson, C.C., 2001. Effective discharge calculation guide. *Int. J. Sediment Res.* 16(4), 445-459.
- Bledsoe, B.P., Hawley, R.J., Stein, E.D. and D.B. Booth. 2010. Hydromodification Screening Tools: Field Manual for Assessing Channel Susceptibility. Southern California Coastal Water Research Project (SCCWRP), Technical Report 606. Costa Mesa, CA. March, 2010. 30 pp.
ftp://ftp.sccwrp.org/pub/download/DOCUMENTS/TechnicalReports/606_HydromodScreeningTools_FieldManual.pdf
- Bledsoe, B.P., Watson, C.C., 2001. Effects of urbanization on channel instability. *J. Am. Water Resour. Assoc.* 37(2), 255-270.
- Booker, F.A., Dietrich, W.E., Collins, L.M., 1993. Runoff and erosion after the Oakland firestorm. *Calif. Geol.* 46, 159-173.
- Booth, D.B., 1990. Stream-channel incision following drainage-basin urbanization. *Water Resour. Bull.* 26(3), 407-417.
- Booth, D.B., 1991. Urbanization and the natural drainage system -- impacts, solutions, and prognoses. *Northwest Environ. J.* 7, 93-118.
- Booth, D.B., 2000. Forest Cover, Impervious-surface Area, and the Mitigation of Urbanization Impacts in King County, Washington. Center for Urban Water Management, University of Washington, Seattle, Wash.
- Booth, D.B., Jackson, C.R., 1997. Urbanization of aquatic systems: degradation thresholds, stormwater detection, and the limits of mitigation. *J. Am. Water Resour. Assoc.* 33(5), 1077-1090.
- Bull, W.B., 1997. Discontinuous ephemeral streams. *Geomorphol.* 19(3-4), 227-276.
- California Forest Service, 1951. Some Aspects of Watershed Management in Southern California. U. S. Department of Agriculture, Forest Service, California Forest and Range Experiment Station, Berkeley, Calif., pp. 28.
- Chin, A., 2006. Urban transformation of river landscapes in a global context. *Geomorphol.* 79(3-4), 460-487.

- Chin, A., Gregory, K.J., 2001. Urbanization and adjustment of ephemeral stream channels. *Ann. Assoc. Am. Geogr.* 91(4), 595-608.
- Chow, V.T., 1964. *Handbook of Applied Hydrology*, McGraw-Hill, Inc., New York, 1467 pp.
- Chow, V.T., Maidment, D.R., Mays, L.W., 1988. *Applied Hydrology*, McGraw-Hill, Inc., New York, 572 pp.
- Coleman, D., MacRae, C., Stein, E.D., 2005. Effect of Increases in Peak Flows and Imperviousness on the Morphology of Southern California Streams. Stormwater Monitoring Coalition, Southern California Coastal Water Research Project, Westminster, Calif.
- Dinicola, R.A., 1989. Characterization and Simulation of Rainfall-runoff Relations for Headwater Basins in Western King and Snohomish Counties, Washington State. Water-Resources Investigation Report 89-4052, U. S. Geological Survey.
- Durbin, T.J., 1974. Digital Simulation of the Effects of Urbanization on Runoff in the Upper Santa Ana River Valley, California. U. S. Geological Survey, Menlo Park, Calif.
- Emmett, W.W., 1975. The Channels and Waters of the Upper Salmon River, Idaho. Professional Paper 870A, U. S. Geological Survey, Washington, D.C.
- Environmental Protection Agency, 2006. Management measures for hydromodification, Chapter 6 in: *Guidance Specifying Management Measures for Nonpoint Pollution in Coastal Waters*. U. S. Environmental Protection Agency.
- Espey, Jr., W.H., Winslow, D.E., 1974. Urban flood frequency characteristics. *Am. Soc. Civil Eng., Proc., J. Hydraul. Div.* 279-293.
- Gabet, E.J., Dunne, T., 2003. A stochastic sediment delivery model for a steep Mediterranean landscape. *Water Resour. Res.* 39(9), 12.
- Galster, J.C., Pazzaglia, F.J., Hargreaves, B.R., Morris, D.P., Stephen, C., Peters, S.C., Weisman, R.N., 2006. Effects of urbanization of watershed hydrology: the scaling of discharge with drainage area. *Geol.* 34(9), 713-716.
- Graf, W.L., 1981. Channel instability in a braided sand-bed river. *Water Resour. Res.* 17, 1087-1094.
- Graf, W.L., 1988. *Fluvial Processes in Dryland Rivers*, Springer-Verlag, Berlin.
- Gregory, K.J., 1976. Drainage networks and climate, in: Derbyshire, E. (Ed.), *Geomorphology and Climate*. Wiley-Interscience, Chichester, pp. 289-315.
- Hack, J.T., 1957. Studies of Longitudinal Stream Profiles in Virginia and Maryland. Professional Paper 294-B, U. S. Geological Survey.
- Hammer, T.R., 1972. Stream channel enlargement due to urbanization. *Water Resour. Res.* 8, 139-167.

- Hawley, R.J., 2009. Effects of Urbanization on the Hydrologic Regimes and Geomorphic Stability of Small Streams in Southern California. Ph.D. Dissertation, Colorado State University, Department of Civil and Environmental Engineering, Fort Collins, Colo., 393 pp.
- Hawley, R.J. and Bledsoe, B.P., 2011. How do flow peaks and durations change in suburbanizing semi-arid watersheds? A southern California case study. *Journal of Hydrology*. <http://dx.doi.org/10.1016/j.jhydrol.2011.05.011>
- Hey, R.D., 1975. Design discharge for natural channels, in: Hey, R.D., Davies, T.D. (Eds.), *Science, Technology and Environmental Management*. Saxon House, pp. 73-88.
- Hollis, G.E., 1975. Effect of urbanization on floods of different recurrence interval. *Water Resour. Res.* 11(3), 431-435.
- Jennings, M.E., Thomas, W.O.J., Riggs, H.C., 1994. Nationwide Summary of U. S. Geological Survey Regionally Regression Equations for Estimating Magnitude and Frequency of Floods for Ungaged Sites, 1993. Water-Resources Investigation Report 94-4002, U. S. Geological Survey, pp. 196.
- Knighton, A.D., 1998. *Fluvial Forms and Processes: A New Perspective*, John Wiley & Sons Ltd., New York, 383 pp.
- Konrad, C.P., Booth, D.B., 2002. Hydrologic Trends Associated with Urban Development for Selected Streams in the Puget Sound Basin, Western Washington. Water-Resources Investigations Report 02-4040, U. S. Geological Survey, Tacoma, Wash.
- Leopold, L.B., 1968. *Hydrology for Urban Land Planning -- A Guidebook on the Hydrologic Effects of Urban Land Use*. Circular 554, U. S. Geological Survey.
- Leopold, L.B., 1994. *A View of the River*, Harvard University Press, Cambridge, Mass., 29 pp.
- Los Angeles County Flood Control District, 1959. Report on Debris Reduction Studies for Mountain Watersheds of Los Angeles County. Los Angeles County Flood Control District, Los Angeles, Calif., pp. 164.
- McPhee, J., 1989. *The Control of Nature*, Farrar, Straus, and Giroux, New York.
- Mooney, D.M., 2007. SIAM -- Sediment Impact Analysis Methods. Ph.D. Dissertation, Colorado State University, Department of Civil and Environmental Engineering, Fort Collins, Colo., 375 pp.
- Novotny, V., 2003. *Water Quality: Diffuse Pollution and Watershed Management*, John Wiley & Sons, New York.
- Pickup, G., Warner, R.F., 1976. Effects of hydrologic regime on magnitude and frequency of dominant discharge. *J. Hydrol.* 29, 51-75.

- Poff, N.L., Bledsoe, B.P., Cuhaciyan, C.O., 2006. Hydrologic variation with land use across the contiguous United States: geomorphic and ecological consequences for stream ecosystems. *Geomorphol.* 79(3-4), 264-285.
- Raff, D.A., Bledsoe, B.P., Flores, A.N., 2004. *GeoTool User's Manual*. Colorado State University, Fort Collins, Colo.
- Rantz, S.E., 1971. *Suggested Criteria for Hydrologic Design of Storm-drainage Facilities in the San Francisco Bay Region, California*. U. S. Geological Survey.
- Roesner, L.A., Bledsoe, B.P., 2002. *Physical Effects of Wet Weather Flows on Aquatic Habitats -- Present Knowledge and Research Needs*. WERF Project Number 00-WSM-4, Water Environment Research Foundation.
- Santa Clara, 2004. *Hydromodification Management Plan Report*. Santa Clara Valley Urban Runoff Pollution Prevention Program, Sunnyvale, Calif.
- Sauer, V.B., Thomas, W.O.J., Stricker, V.A., Wilson, K.V., 1983. *Flood Characteristics of Urban Watersheds in the United States*. U. S. Geological Survey.
- Schumm, S.A., 1991. *To Interpret the Earth: Ten Ways to be Wrong*, Cambridge University Press, 133 pp.
- Simon, A., Downs, P.W., 1995. An interdisciplinary approach to evaluation of potential instability in alluvial channels. *Geomorphol.* 12, 215-232.
- Strahler, A.N., 1952. Hypsometric analysis of erosional topography. *Geol. Soc. Am. Bull.* 63, 1117-1142.
- Trimble, S.W., 1997. Contribution of stream channel erosion to sediment yield from an urbanizing watershed. *Sci.* 278, 1442-1444.
- U. S. Army Corps of Engineers, 2009. *HEC-RAS 4.0. Hydrologic Engineering Center - River Analysis System*, Davis, Calif.
- U. S. Water Resources Council, 1967. *A Uniform Technique for Determining Flood Flow Frequencies*. Bulletin 15 of the Hydrology Subcommittee, U.S. Water Resources Council, Washington, D.C., pp. 15.
- U. S. Water Resources Council, 1981. *Guidelines for Determining Flood Flow Frequency*. Bulletin 17B of the Hydrology Subcommittee, U.S. Water Resources Council, Washington, D.C., pp. 28.
- Urbonas, B.R., Roesner, L.A., 1993. Hydrologic design for urban drainage and flood control, in: Maidment, D.R. (Ed.), *Handbook of Hydrology*. McGraw-Hill, New York, pp. 28.1-28.52.
- Waananen, A.O., 1969. Urban effects on water yield, in: Moore, W.L., Morgan, C.W. (Eds.), *Water Resources Symposium* University of Texas Press, pp. 169-182.

- Waananen, A.O., Crippen, J.R., 1977. Magnitude and frequency of floods in California. U. S. Geological Survey.
- Waters, T.F., 1995. Sediment in streams -- sources, biological effects, and control. Am. Fish. Soc. Monograph 7, 251.
- Watson, C.C., Dubler, D., Abt, S.R., 1997. Demonstration Erosion Control Project Report. CSU Report submitted to U.S. Army Engineer Waterways Experiment Station, Vicksburg, Miss.
- Williams, G.P., 1978. Bank-full discharge of rivers. Water Resour. Res. 14(6), 1141-1154.
- Wolman, M.G., Gerson, R., 1978. Relative scales of time and effectiveness of climate in watershed geomorphology. Earth Surf. Process. 3, 189-208.
- Wolman, M.G., Miller, J.P., 1960. Magnitude and frequency of forces in geomorphic processes. J. Geol. 68, 54-74.
- Yevjevich, V., 1972. Probability and Statistics in Hydrology, Water Resources Publications, Fort Collins, Colo., 302 pp.

Internet References – GIS Data Sources

- Cal-Atlas:** *2000 and 2007 Roadway Shapefiles*, State of California Geospatial Clearinghouse, <http://www.atlas.ca.gov>.
- Google Earth:** *Present-day Aerial Photography*, <http://earth.google.com>.
- National Oceanic and Atmospheric Administration:** *Precipitation Intensities for 2-year, 24-hour Storm*, <http://www.nws.noaa.gov/oh/hdsc/noaaatlas2.htm> (Atlas 2), National Weather Service, Hydrometeorological Design Studies Center; and hdsc.nws.noaa.gov/hdsc/pfds/pfds_gis.html (Atlas 14), National Weather Service, Hydrometeorological Design Studies Center, Precipitation Frequency Data Server.
- U. S. Department of Agriculture, Natural Resources Conservation Service:** *Soil Surveys, Average Annual Precipitation Shapefile (1961 - 1990)*, <http://datagateway.nrcs.usda.gov/>, Geospatial Data Gateway.
- U. S. Geological Survey:** *Historical Aerial Photography and Quadrangle Topographic Maps, National Elevation Dataset, 2001 Impervious Raster, National Hydrography Dataset, Average Annual Precipitation Shapefile (1900 - 1960)*, <http://seamless.usgs.gov>, The National Map Seamless Server.